REPORT DOCUMENTATION PAGE

Form Approved
OMB No. 0704-0188

1. REPORT DATE *(DD-MM-YYYY)*	**2. REPORT TYPE**	**3. DATES COVERED** *(From - To)*
August 2013	Technical Paper	August 2013-October 2013

4. TITLE AND SUBTITLE
Time-Synchronized CW-Laser Induced Fluorescence Velocity Measurements of a Diverging Cusped Field Thruster

5a. CONTRACT NUMBER
In-House

5b. GRANT NUMBER

5c. PROGRAM ELEMENT NUMBER

6. AUTHOR(S)
Natalia A. MacDonald, Landon J. Tango, William A. Hargus, Jr., and Mark A. Cappelli

5d. PROJECT NUMBER

5e. TASK NUMBER

5f. WORK UNIT NUMBER
Q09W

7. PERFORMING ORGANIZATION NAME(S) AND ADDRESS(ES)

Air Force Research Laboratory (AFMC)
AFRL/RQRS
1 Ara Drive.
Edwards AFB CA 93524-7013

8. PERFORMING ORGANIZATION REPORT NO.

9. SPONSORING / MONITORING AGENCY NAME(S) AND ADDRESS(ES)
Air Force Research Laboratory (AFMC)
AFRL/RQR
5 Pollux Drive
Edwards AFB CA 93524-7048

10. SPONSOR/MONITOR'S ACRONYM(S)

11. SPONSOR/MONITOR'S REPORT NUMBER(S)
AFRL-RQ-ED-TP-2013-219

12. DISTRIBUTION / AVAILABILITY STATEMENT
Distribution A: Approved for Public Release; Distribution Unlimited. PA#13511

13. SUPPLEMENTARY NOTES
Conference paper for the International Electric Propulsion Conference 2013, Washington, D.C., 6-10 October 2013.

14. ABSTRACT
New measurements are presented of time-synchronized ion velocities at several points in the channel and plume of a diverging cusped field thruster operating on xenon. Xenon ion velocities for the thruster are derived from laser-induced fluorescence measurements of the $5d[4]_{7/2} - 6p[3]_{5/2}$ xenon ion excited state transition centered at _ = 834.72 nm. The thruster is operated in a high current mode, where the anode discharge current is shown to oscillate quasi-periodically. A sample-hold scheme is implemented to correlate ion velocities to phases along the current cycle. These time-synchronized measurements show that both the most probable ion velicities and the widths of ion velocity distributions vary in a way that is correlated to the DCFT's discharge current.

15. SUBJECT TERMS

16. SECURITY CLASSIFICATION OF:			**17. LIMITATION OF ABSTRACT**	**18. NUMBER OF PAGES**	**19a. NAME OF RESPONSIBLE PERSON**
					William Hargus
a. REPORT	**b. ABSTRACT**	**c. THIS PAGE**	SAR	52	**19b. TELEPHONE NO** *(include area code)*
Unclassified	**Unclassified**	**Unclassified**			661-525-6799

Standard Form 298 (Rev. 8-98)
Prescribed by ANSI Std. 239.18

Time-Synchronized CW-Laser Induced Fluorescence Measurements of a Diverging Cusped Field Thruster

Natalia A. MacDonald, Landon J. Tango and William A. Hargus, Jr.
In-Space Propulsion Branch
Air Force Research Laboratory
Edwards AFB, CA 93524

Mark A. Cappelli
Stanford Plasma Physics Laboratory
Stanford University
Stanford, CA 94305

New measurements are presented of time-synchronized ion velocities at several points in the channel and plume of a diverging cusped field thruster operating on xenon. Xenon ion velocities for the thruster are derived from laser-induced fluorescence measurements of the $5d[4]_{7/2} - 6p[3]_{5/2}$ xenon ion excited state transition centered at $\lambda = 834.72$ nm. The thruster is operated in a high current mode, where the anode discharge current is shown to oscillate quasi-periodically. A sample-hold scheme is implemented to correlate ion velocities to phases along the current cycle. These time-synchronized measurements show that both the most probable ion velicities and the widths of ion velocity distributions vary in a way that is correlated to the DCFT's discharge current.

I. Introduction

As the satellite community attempts to reduce spacecraft size and cost, scaling of appropriate propulsion devices such as Hall thrusters has become of particular interest. Alongside the development of new propulsion technologies comes the need for advanced diagnostic capabilities to understand the dynamics of thruster operation. This work describes the implementation and continued use of a time-synchronized method of Laser-Induced Fluorescence (LIF) velocimetry. The time-synchronized LIF method is applied to the Massachusetts Institute of Technology (MIT) developed Diverging Cusped Field Thruster (DCFT) in an effort to better understand ion acceleration mechanism.

The DCFT was developed in an effort to mitigate issues such as increased heat flux and sputtering to channel walls that arise when scaling down Hall thrusters in power.[1,2] The DCFT tends to operate in two modes: a high current mode, characterized by quasi-periodic discharge current oscillations; and a low current mode that is quiescent.[3] These two modes of operation have been diagnosed with time-averaged LIF velocimetry.[4] Differences in the time-averaged velocity maps between the two modes include the presence of a widely distributed acceleration region and diffuse plume during the high current mode that are not present in the low current mode. While time-averaged measurements provide a good representation of the ion velocities throughout a quiescent discharge, the differences in the velocity maps may be indicative of additional ion dynamics in the oscillatory mode of operation that can only be resolved with a time-dependent velocity diagnostic.

Xenon ion LIF velocity measurements are achieved by probing the $5d[4]_{7/2} - 6p[3]_{5/2}$ xenon ion excited state transition with a continuous wave (CW) laser centered at $\lambda = 834.72$ nm. To achieve time-synchronization with the CW laser, a sample-hold scheme is implemented. In this scheme, an AC measure-

ment of the DCFT's discharge current and a comparator are used to trigger the sampling function of a boxcar averager at points where the discharge passes through zero. The boxcar samples and holds the value of the thruster's emission plus flouorescence trace at each subsequent trigger. The resulting sample-held signal is passed through a lock-in amplifier for phase sensitive detection. By triggering the time-synchronization on the discharge current's zero point crossing rather than frequency, this method allows for jitter in the frequency of the discharge (i.e. the oscillations can be quasi-periodic).

The new measurements presented in this work explore time-synchronized ion velocities at additional positions within the plume of the DCFT that have not been previously reported. These measurements provide a better understanding of the acceleration mechanism in the high current mode of operation of the DCFT.

II. Experiment

A. Diverging Cusped Field Thruster

Figure 1a provides a schematic of the DCFT. The acceleration channel in the DCFT has a diverging, cone shape that is lined with permanent samarium cobalt (SmCo) magnets of alternating polarity. These magnets create a cusped magnetic field profile that is largely in the axial direction, with radial components at the magnet interfaces. Details of this design have been described extensively elsewhere.[5]

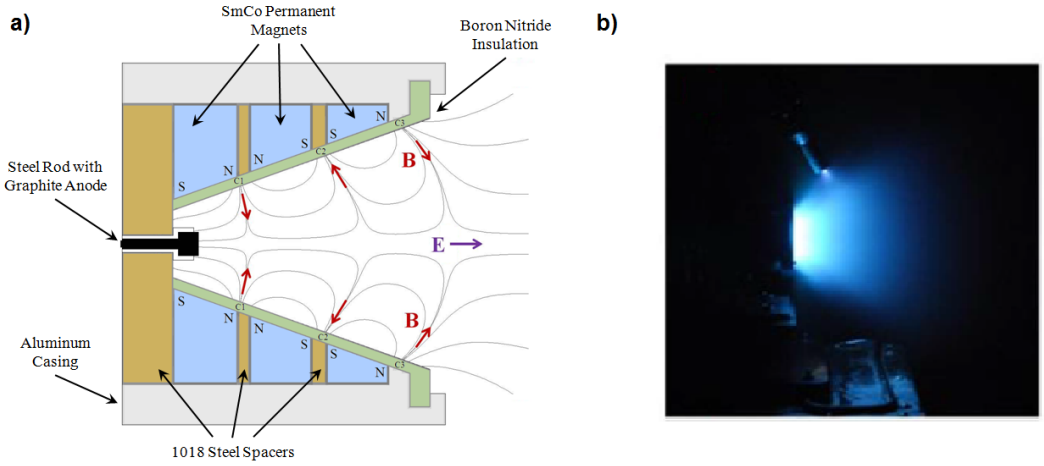

Figure 1. Diverging Cusped Field Thruster, developed by MIT. a) Schematic of DCFT, b) Operation in high current mode.

Table 1. DCFT operating condition during time-synchronized measurements.

Anode Flow	830 $\mu g/s$ Xe (8.5 sccm)
Cathode Flow	150 $\mu g/s$ Ar (4.75 sccm)
Anode Potential	300 V
Anode Current	0.49 A
Keeper Current	0.50 A
Heater Current	7.0 A

The DCFT tends to operate in either a high current or low current mode. The high current mode is characterized by periodic oscillations in the discharge current, while the low current mode is quiescent. This work focuses on the high current mode, shown Fig. 1b, with the operating condition described in Table 1. The oscillatory nature of the high current mode has been attributed to three distinguishable phases within

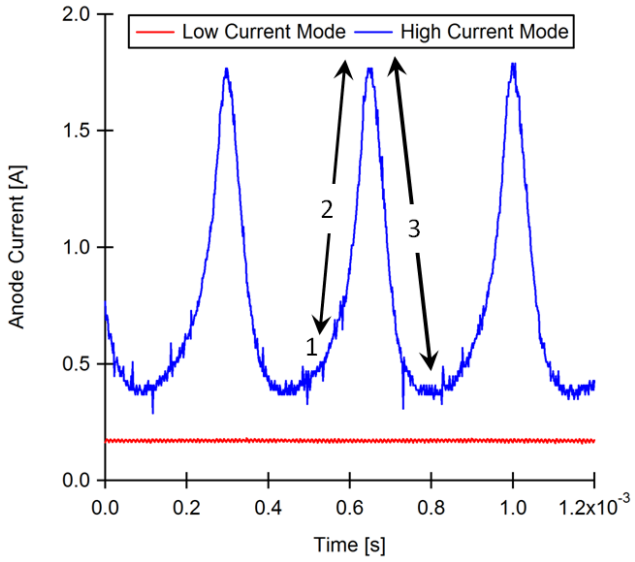

Figure 2. Anode current traces for both the low and high current operating modes of the DCFT. Numbers 1 to 3 on the high current trace describe the three phases within the oscillatory mode's current cycle.

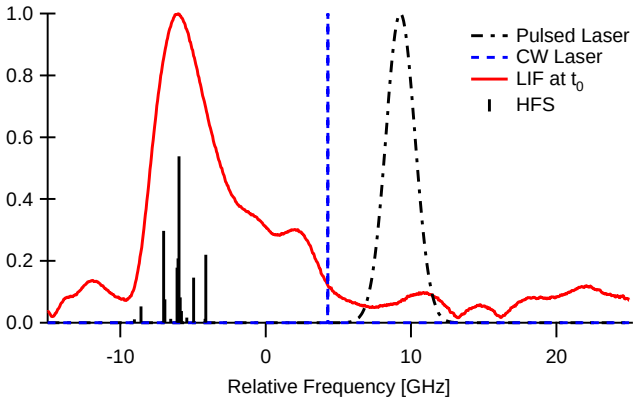

Figure 3. Fluorescence excitation lineshape at time t_0 at a position $X = -8$ mm, $Z = 0$ mm at the exit plane of the DCFT, as compared to the width of a typical CW laser and a pulsed dye laser. The hyperfine structure (HFS) of the transition is shown for reference.

each current cycle: (1) Fast ionization of neutrals; (2) Evacuation of ions from the downstream end of the formed plasma, with simultaneous electron evacuation to the anode; and (3) Gradual re-fill of neutrals in the thruster channel. These phases are depicted in Fig. 2. This thruster has shown great promise for operation in the <200 W power regime, with anode efficiencies on the order of 40%.[6] Under the operating conditions in this work, the DCFT operates at an average power of 147 W.

B. Motivation

Pulsed dye lasers are typically employed in time-resolved LIF measurements to determine properties such as the temperature, velocity distribution etc. of a discharge. However, the spectral linewidths of the xenon ion transition examined in this work are too narrow to be resolved with pulsed dye lasers. The $5d[4]_{7/2} - 6p[3]_{5/2}$ xenon ion transition has a measured linewidth (a convolution of the natural linewidth of the transition and the velocity distribution function (VDF)) on the order of 1.5 to 2.5 GHz. Cutting edge pulsed dye lasers have linewidths of >1 GHz[7] at best. In comparison, CW lasers with linewidths <300 kHz[7] are sufficiently narrow to resolve the transition's spectral features, and are therefore more desirable for making time-synchronized fluorescence measurements.

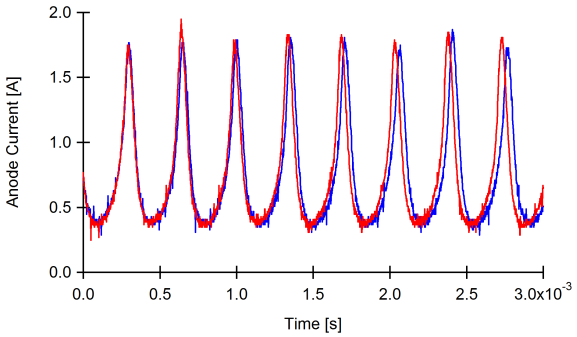

Figure 4. DCFT current traces, taken approximatly 30 seconds apart during the same laser scan. Note the slight shift in frequency.

Figure 3 provides a fluorescence excitation lineshape for time t_0 at a position of $X = -8$ mm, $Z = 0$ mm at the exit plane of the DCFT. The linewidths for a CW and a pulsed dye laser, as well as the hyperfine structure (HFS) of the probed transition are also shown for reference. These line widths illustrate the need for a CW laser when resolving this spectral feature.

Some previous studies have employed CW lasers in time-resolved LIF measurements to diagnose oscillatory plasma discharges from Hall thrusters.[8,9] However, the oscillatory discharge has been regulated at a particular frequency by a variable cathode current injection, periodic disruptions to the discharge power, etc. Our method is uniquely designed for use on discharges with quasi-periodic oscillations, without any regulation of the naturally occurring oscillation frequency.

Figure 4 provides discharge current traces for the DCFT, taken approximately 30 seconds apart during the same laser scan. This figure illustrates the jitter in the DCFT discharge frequency that makes a sample-hold/lock-in scheme attractive. For a CW laser modulated by a mechanical chopper with a 50% duty cycle, the time-domain addition and subtraction of gated integration requires averaging over a large number of signal on/off cycles to achieve similar results to the frequency domain filtering of phase sensitive detection. By implementing a phase sensitive detection that is connected to a fixed chopper frequency, and a sample-hold circuit that triggers a time-synchronization when the current discharged from the DCFT passes through a certain level, not frequency, we are able to extract fluorescence signals correlated to discharge currents that are not perfectly periodic.

C. Experimental Apparatus

Measurements are performed in in Chamber 6 of the Air Force Research Laboratory (AFRL) Electric Propulsion Laboratory at Edwards AFB, CA. Chamber pressure during thruster operation is approximately 2.8×10^{-6} torr. The results of these measurements are compared to a previous test campaign performed in the large vacuum chamber facility at the Stanford Plasma Physics Laboratory (SPPL).[12]

Ion velocity measurements are accomplished by probing the $5d[4]_{7/2} - 6p[3]_{5/2}$ electronic transition of Xe II at 834.72 nm. The lower state of this transition is metastable, while the upper state is shared by the $6s[2]_{3/2} - 6p[3]_{5/2}$ transition at 541.92 nm,[13] which is used in this study for non-resonant fluorescence collection. This transition has been used extensively throughout the electric propulsion community for time-averaged LIF velocimetry measurements,[14–17] including previous work on the DCFT.[4] Ion velocities are determined by measuring the Doppler shift of the absorbing ions.[18]

Figure 5 depicts the LIF optical system. The lower portion shows the probe optics before they enter the vacuum chamber. The laser is a New Focus Vortex $TLB - 6017$ tunable CW diode laser, with a center wavelength of 834.7 nm. The laser is typically scanned over an ∼20 GHz frequency range to encompass an entire spectral feature as well as a nearby reference line. The 10 mW beam is passed through several beam pick-offs for diagnostic purposes. The first beam pick-off directs a beam to a photodiode detector (D1) used to provide constant power feedback to the laser. The second beam is divided into two equal components by a 50-50 cube beam splitter. The first component is directed to a Burleigh WA-1500 wavelength meter used to monitor absolute wavelength. The second component is sent through a low pressure xenon hollow cathode discharge lamp (HCL), that provides a wavelength reference through absorption of the neutral xenon $6s'[1/2]_1^0 - 6p'[3/2]_2$ transition at 834.68 nm.[19,20] The second pick-off sends a beam to a 300 MHz

free spectral range Fabry-Perot etalon (F-P) that provides high resolution relative frequency monitoring of the wavelength during a laser scan.

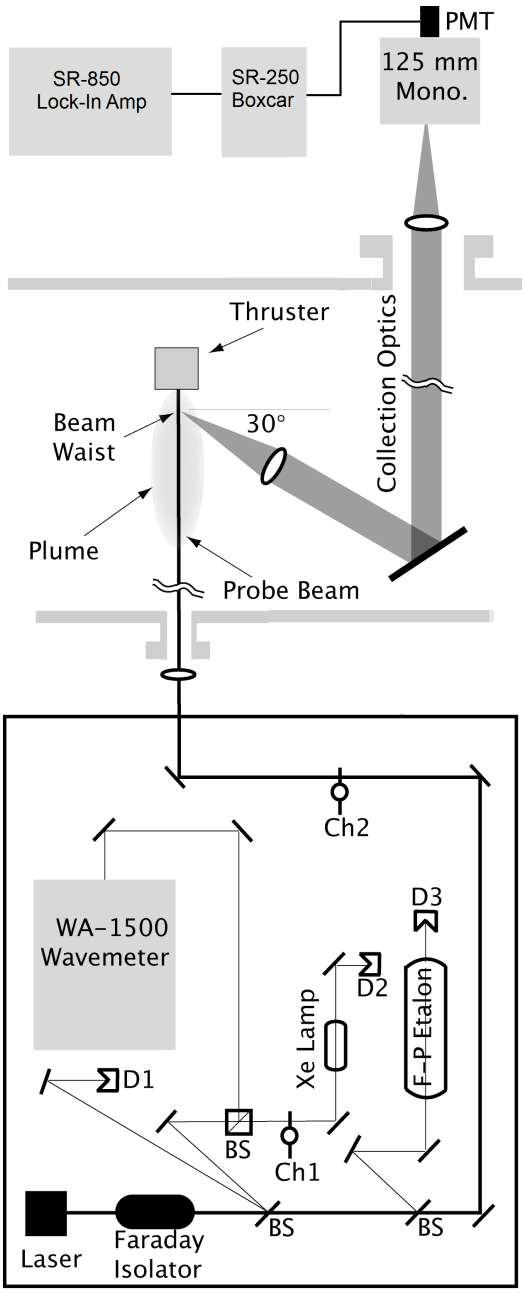

Figure 5. Top view diagram of the laser optical train and collection optics for time-synchronized thruster LIF measurements at SPPL. BS = Beam Splitter; Ch = Chopper; D = Diode; L = Lens; M = Mirror.

The main portion of the beam is sent through a Stanford Research Systems SR540 mechanical chopper, rotating at 400 Hz for phase sensitive detection. Once inside the vacuum chamber, the beam is directed such that it probes axial ion velocities in the thruster. The fluorescence signal is collected by a 100 mm diameter plano-convex lens with a focal length of 250 mm. This lens is oriented 30° from the exit plane, a distance of 250 mm from the intersection with the probe beams, to minimize interactions with the plume (i.e. sputtering on the optics). The collected light exits the vacuum chamber and is focused into a 125 mm focal length monochromator with a photomultiplier tube (PMT) by a second 100 mm diameter plano-convex lens with a focal length of 250 mm. The collection optics have a 1:1 magnification, which allows the spatial resolution of the measurements to be determined by the diameter of the probe beam (1 mm) and the image

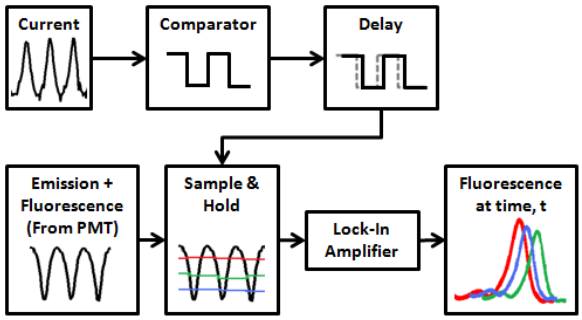

Figure 6. Block diagram of the sample-hold method of synchronizing the fluorescence trace to various times along a discharge current cycle.

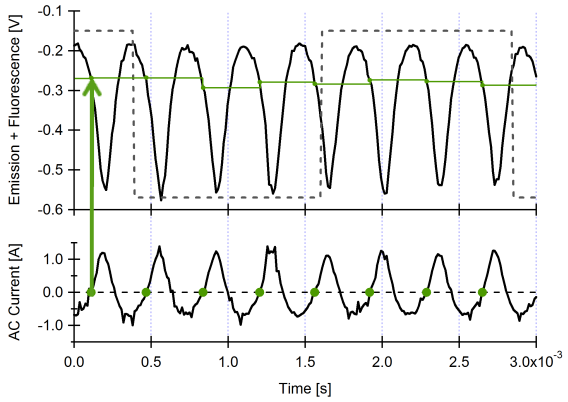

Figure 7. Raw PMT and AC current traces for the DCFT discharge. Arrow indicates the correlation between points in current cycle (bottom) and sample-held signal from the emission plus fluorescence trace (top) for time = t_0. Chopper frequency (- - -) is shown for reference. Note: the emission plus fluorescence signal is negative due to the negatively applied bias on the PMT.

of the entrance slit (0.8 mm width by 0.2 mm height) that defines the collection optics solid angle. If sent directly into a lock-in amplifier, the resulting signal would be a conventional time-averaged measurement of the fluorescence excitation lineshape.

To synchronize the LIF signal in time to the discharge current, a sample-hold scheme is implemented between the PMT and the lock-in amplifier. The development of this sample-hold scheme, as well as initial results for the DCFT, are described elsewhere.[12,21,22] Fig. 6 provides a block diagram of the sample-hold method. Simultaneous measurements are made of the AC discharge current, absorption reference, etalon, and emission plus fluorescence signal from the PMT, as the CW laser is scanned slowly in wavelength across the spectral feature. Due to the large background emission and associated noise, laser scans typically take on the order of 30 minutes to achieve adequate signal-to-noise for the fluorescence excitation lineshape.

The AC measurement of discharge current is fed into an LM339 comparator. Points where the current passes through zero with a positive slope trigger the comparator, resulting in a series of transistor-transistor logic (TTL) pulses with an approximately 50% duty cycle. The comparator signal and raw emission plus fluorescence signal from the PMT are then fed into an SRS SR-250 Boxcar Averager where the sample-hold function is performed.

For every positive slope in the comparator signal, the boxcar averager samples the PMT signal for a period of time defined by the gate width. The last sampled value of the PMT signal is held until the next comparator trigger, at which point the boxcar averager re-samples and holds the PMT signal. Fig. 7 provides an example of how the zero point crossings of the AC discharge current correlate to points in the sample-held emission plus fluorescence signal. This process is repeated throughout the length of the laser scan, resulting in the "sample-held" signal, shown in green.

The sample-held signal is then fed into an SRS SR-850 Lock-in Amplifier with the chopper reference frequency for phase sensitive detection, resulting in a fluorescence excitation lineshape synchronized to time

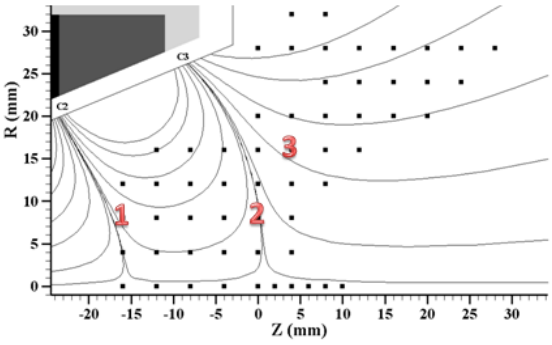

Figure 8. Positions of the three time-synchronized LIF measurements on the DCFT.

t_0 in the current discharge cycle. To sample additional times along the current cycle, an SRS DG535 digital delay generator is used to adjust the sample trigger before the laser scan is repeated.

III. Results and Discussion

Figure 8 provides the three measurement locations used in the time-synchronized study of the DCFT. These points were chosen based on the time-averaged DCFT velocity measurements presented in previous work.[4] In these measurements, the DCFT's high current mode revealed axial acceleration beginning as deep as Z = -12 to -16 mm in the thruster channel (near the second cusp). This is in contrast to the quiescent, low current mode of operation, in which the majority of ion acceleration was localized just inside the thruster exit plane (near the third cusp).

From these observations, Point 1 was chosen because it is in the brightest region of the plume, and is likely near a region of high ionization inside the thruster channel. This point is located at R = +8 mm, Z = -16 mm, inside the thruster channel near the separatrix defined by the second cusp, marked as C2. Point 2, at R = +8 mm, Z = 0 mm, is at the exit plane of the thruster near the outermost separatrix defined by the third cusp, C3. This point is near the region of highest measured potential drop, where the majority of ion acceleration begins. Point 3, at R = +16 mm, Z = +4 mm, is after the majority of the potential drop, where time-averaged measurements indicate that the ions continue ballistically outward, perpendicular to the separatrix at cusp C3.

Figure 9 provides a contour plot of the time-synchronized ion velocity distributions at the exit plane of the thruster (Point 2). This contour plot was achieved by interpolating lineshapes that were measured at twelve points in time along the current cycle. These points are shown as horizontal dashed lines across the figure. Note that measurements were not taken between 100-200 μs due to limitations in triggering the sample-hold circuit, and interpolated results between these times should therefore be interpreted with caution.

The three lineshapes on the right of Fig. 9 show ion velocity distributions that are typical of different phases along the current cycle at Point 2. At the begining of the current cycle, the lineshape is relatively narrow and the most probable (peak) velocities are on the order of 5 km/s. As the current reaches its peak, a second peak forms in the velocity distribution, indicating the presence of near zero and negative velocity ions. As the current cycle progresses, this second peak diminishes until the distribution once again resembles that of the begining of the current cycle.

Figures 10 to 12 summarize the most probable velocities and the full-widths at half maximum (FWHMs) for the three measurement locations described in this work. At each of the measurement locations, the most probable velocities decline and reach their minimum as the discharge current is at its maximum. At point 1, in the ionization region, the velocities are low and there appears to be no additional correlation between the widths of the velocity distributions and the current cycle. At point 2, the widths of the velocity distributions increase with increasing discharge current, primarily due to the aforementioned second peak of lower velocity ions. A similar correlation is seen at point 3.

In time-averaged measurements, both the high and low current modes of operation result in a velocity of approximately 5-6 km/s along the contour of the ourtermost cusp (near the exit plane).[4] However, further

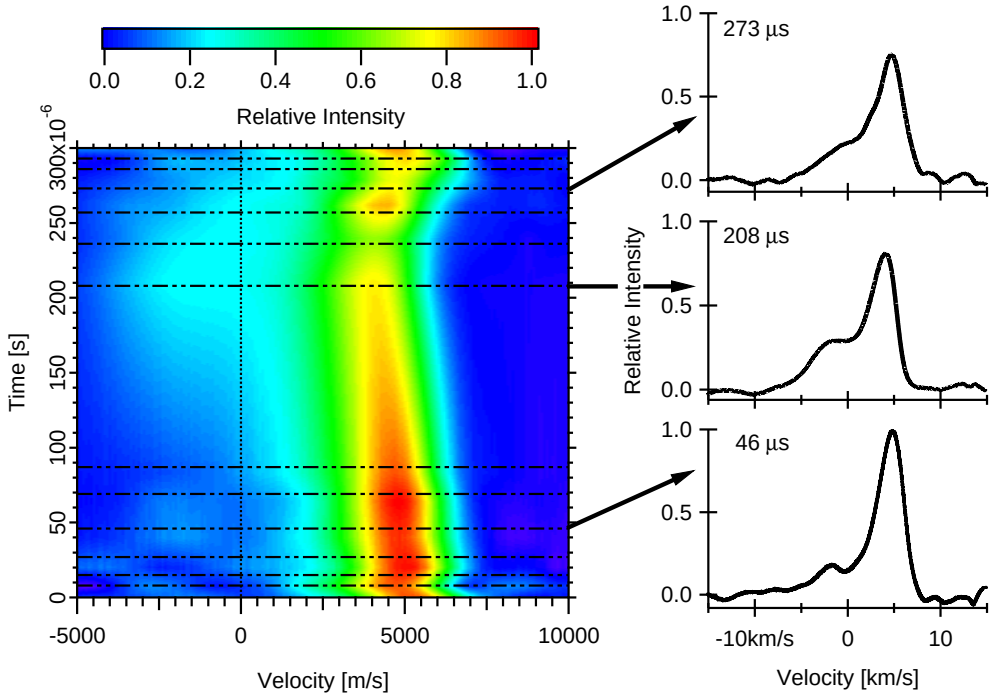

Figure 9. Variation of the ion velocity distributions for a single current cycle, measured at the exit plane of the DCFT, X = -8 mm, Z = 0 mm. Individual velocity distributions are shown for three phases of the current cycle (right), while the contour plot (left) shows the velocity distributions interpolated over the entire current cycle. Dashed lines (— – –) represent measurement times.

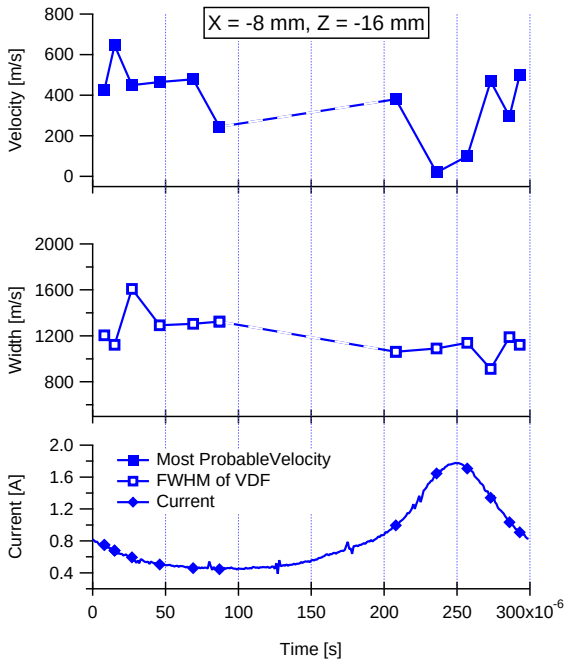

Figure 10. Measured most-probable axial ion velocities and full-widths at half maximum (FWHMs) of the measured velocity distributions as a function of the DCFT's discharge current at Z= -16 mm, X = -8 mm.

comparion revealed that in the low current, quiescent mode, the majority of ion acceleration was localized just inside the thruster exit plane (near the third cusp), while the oscillatory, high current mode had axial

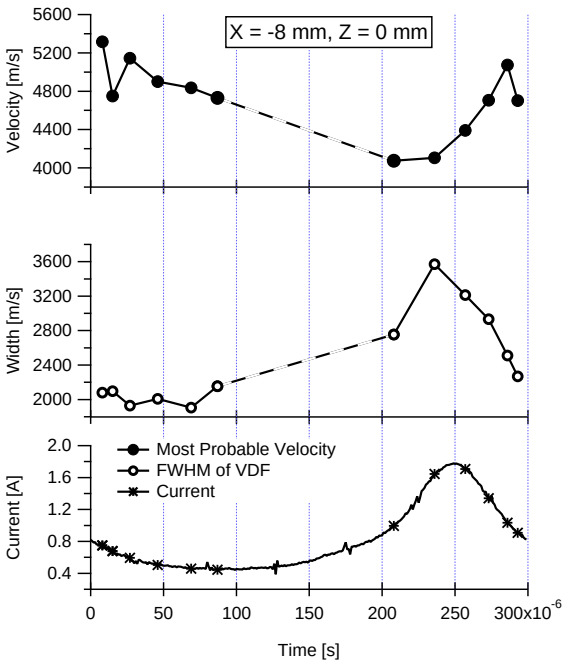

Figure 11. Measured most-probable axial ion velocities and full-widths at half maximum (FWHMs) of the measured velocity distributions as a function of the DCFT's discharge current at Z = 0, X = -8 mm.

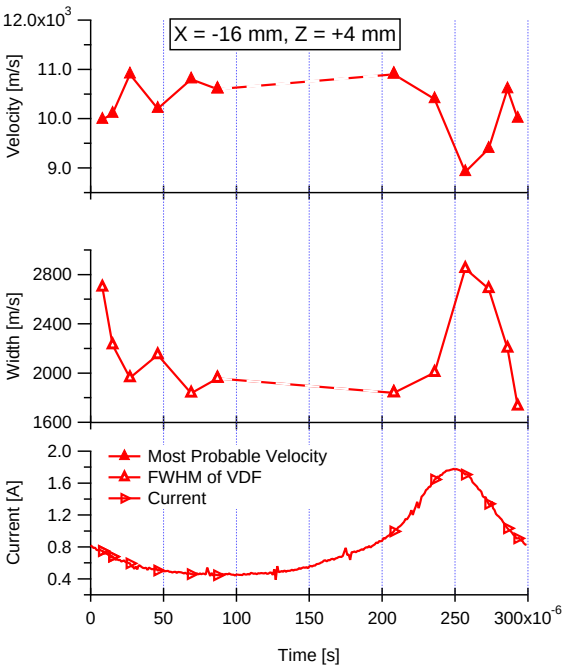

Figure 12. Measured most-probable axial ion velocities and full-widths at half maximum (FWHMs) of the measured velocity distributions as a function of the DCFT's discharge current at Z = +4 mm, X = -16 mm.

acceleration distributed at least as deep as Z = -16 mm in the thruster channel (near the second cusp).

Assuming that ions are born in a relatively fixed volume near point 1, the wider distribution of the position of the high current mode's initial acceleration may indicate a fluctuation of the position of the peak electric field. Let us assume that the peak electric field, and thereby steepest potential drop, moves outwards in position as the discharge current reachess its peak, then recedes back towards Z = -5 mm as the current

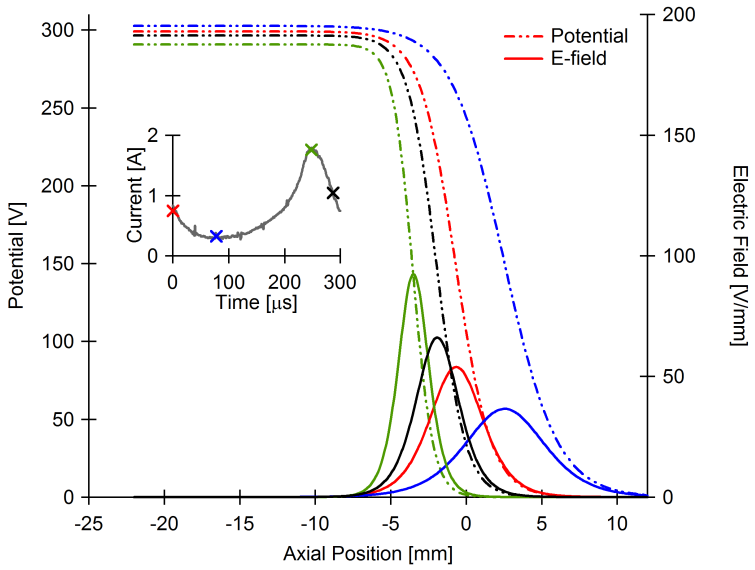

Figure 13. Theorized correlation between DCFT current cycle and position of and potential drop/electric field.

decreases. This theory is depicted in Fig. 13.

Early in the current cycle, the ion velocities at point 1 are slightly higher, corresponding to times when the wings of the electric field curve reach back to Z = -16 mm. When the current increases, and the electric field moves outwards, the ions measured remain near the thermal velocity at which they were born. Because the ion velocities are relatively low, the probed ions are likely to originate from virtually the same point (or a small subsection) of the ionization region. These ions would then experience the same acceleration, resulting in the FWHMs of the ion velocity distribution being relatively constant over the course of a current cycle.

At points 2 and 3, the probed ions have experienced successively larger portions of the acceleration due to the applied potential drop. Similar to point 1, when the potential drop is inside the thruster channel, ions at the measurement location have experienced a greater portion of their acceleration compared to when the potential drop moves outwards. At point 2, the resulting ion velocities reach there maximum around 5 km/s and their minimum of 4.2 km/s. At point 3, the maximum most probable ion velocity reached is 11 km/s, and the minimum at this point is 8.9 km/s.

In contrast to point 1, the FWHMs of the velocity distributions at points 2 and 3 change in phase with the changing discharge current. The changing FWHMs could be attributed ions born at different times in the current cycle or at different positions within the ionization volume. In the case of point 2, the formation of a secondary velocity peak between 200-250 μs shown in Fig. 9 could be due to the ions born closer to the exit plane of the thruster. For the slower moving ions, the movement of the potential drop back and forth over the measurement point may induce some backwards movement of the ions, as is indicated by the small negative velocitiy population in the distributions at these times. As the peak electric field recedes back inside the exit plane, the width of the velocity distribution decreases, as does the negative velocity ion population.

Point 3 shows a similar pattern, but instead of a distinct second peak forming, the primary peak widens and narrows with changing current. At this point, the spread between maximum and minimum FWHMs is slightly larger, at 1.9 km/s to 3.6 km/s versus the 1.8 km/s to 2.8 km/s spread seen at point 2.

IV. Conclusions

A sample-hold with phase sensitive detection method of time-synchronized CW laser-induced fluorescence was presented. Time-synchronized ion velocity measurements were made at three points in the plume of the DCFT, operating in its oscillatory high-current mode. These measurements revealed that ion velocities in the DCFT are directly correlated to the phase of the discharge current oscillations, whereas the time-averaged

velocity measurements were unable to resolve these dynamics.

At point 1, in the ionization region of the DCFT, most probable ion velocities deacreased as the discharge current reached its peak. The widths of the ion velocity distributions remained relatively constant in this region. At points 2 and 3, at the exit plane and farther into the plume, most probable ion velocities also showed a deacrease as the discharge current reached its peak. In these regions, there was also a correlation between the widths of the ion velocity distributions, which increased as the discharge current increased.

These time-synchronized velocity measurements support the theory that the peak electric field oscillates in position across the exit plane of the thruster. Further measurements are underway to continue to build a better understanding fo these discharge oscillations.

Acknowledgments

This research at Stanford and the Air Force Research Laboratory is funded through the Air Force Office of Scientific Research with Dr. M. Birkan as grant monitor.

V. References

References

[1]V. Khayms and M. Martinez-Sanchez. *Design of a miniaturized Hall thruster for microsatellites: Proceedings of the 32nd AIAA, ASME, SAE, and ASEE, Joint Propulsion Conference and Exhibit,* Lake Buena Vista, FL, July 1-3, 1996, AIAA-96-3291.

[2]D. P. Schmidt, N. B. Meezan, W. A. Hargus, Jr., and M. A. Cappelli. Plasma Sources Sci. Technol. **9**, 68 (2000).

[3]S. R. Gildea and T. S. Matlock and P. Lozano and M. Martinez-Sanchez *Low Frequency Oscillations in the Diverging Cusped-Field Thruster: Proceedings of the 46th AIAA/ASME/SAE/ASEE Joint Propulsion Conference & Exhibit,* Nashville, TN, July 25-28, 2010, AIAA-2010-7014.

[4]N. A. MacDonald, M. A. Cappelli, S. R. Gildea, M. Martinez-Sanchez, and W. A. Hargus Jr. J. Phys. D **44**, 295203 (2011).

[5]D. G. Courtney and P. Lozano and M. Martinez-Sanchez. *Continued Investigation of Diverging Cusped Field Thruster: Proceedings of the 44th AIAA/ASME/SAE/ASEE Joint Propulsion Conference & Exhibit,* Hartford, CT, July 21-23, 2008, AIAA 2008-4631.

[6]D. G. Courtney, and M. Martinez-Sanchez. *Diverging Cusped-Field Hall Thruster (DCHT): Proceedings of the 30th International Electric Propulsion Conference,* Florence, Italy, September 17-20, 2007, IEPC-2007-39.

[7]Newport Corporation. Website. Accessed: 16 December 2011. http://www.newport.com.

[8]S. Mazouffre, D. Gawron, and N. Sadeghi. Phys. of Plasmas **16**, 1 (2009).

[9]S. Mazouffre Plasma Sources Sci. Technol. **22**, 013001 (2013).

[10]J. P. Boeuf and L. Garrigues. J. Appl. Phys. **84**, 3541 (1998).

[11]E. Y. Choueiri. Phys. Plasmas **8**, 1411-1426 (2001).

[12]N. A. MacDonald, M. A. Cappelli and W. A. Hargus Jr. J. Phys. D Pre-print (2013).

[13]J. E. Hansen, and W. Persson. Phys. Scr. **4**, 602 (1987).

[14]N. A. MacDonald, C. V. Young, M. A. Cappelli, and W. A. Hargus, Jr. J. Appl. Phys. **111**, 093303 (2012).

[15]D. H. Manzella. *Stationary Plasma Thruster Ion Velocity Distribution: Proceedings of the 30th AIAA/ASME/SAE/ASEE Joint Propulsion Conference & Exhibit,* Indianapolis, IN, June 27-29, 1994, AIAA-1994-3141.

[16]Hargus, Jr., W. A. and M. A. Cappelli. Appl. Phys. B **8**, 961 (2001).

[17]S. Mazouffre, D. Gawron, V. Kulaev, and N. Sadehgi. IEEE Trans. Plasma Sci. **36**, 1967 (2008).

[18]W. Demtroder, *Laser Spectroscopy: Basic Concepts and Instrumentation* (Springer-Verlag, Berlin, 1996).

[19]M. H. Miller, and R. A. Roig. Phys. Rev. A **8**, 480 (1973).

[20]C. E. Moore. *Atomic Energy Levels. vol. II* (National Bureau of Standards, Gaithersburg, MD, 1958).

[21]N. A. MacDonald and M. A. Cappelli and W. A. Hargus Jr. *Development of a Time Synchronized CW-Laser Induced Fluorescence Measurement for Quasi-Periodic Oscillatory Plasma Discharges: Bulletin of the 65th Annual Gaseous Electronics Conference,* Austin, TX, October 22-26, 2012, Vol. 57, No. 8.

[22]N. A. MacDonald, M. A. Cappelli, and W. A. Hargus Jr. Rev. Sci. Instrum. **83**, 113506 (2012).

Air Force Research Laboratory

Time Synchronized CW-Laser Induced Fluorescence Measurement for Quasi-Periodic Oscillatory Plasma Discharges

Date: 20 August 2013

Natalia A. MacDonald, PhD
Landon J. Tango
William A. Hargus, PhD
AFRL/RQRS

Prof. Mark Cappelli
Stanford Plasma Physics Laboratory

AFRL

Outline

- Introduction
  - Motivation for research
  - Laser Induced Fluorescence (LIF) velocimetry
- Approaches to Time-Synchronization
  - Pulsed vs. CW Laser
  - Digital Sample-Hold Method
  - Hardware Sample-Hold Method
- Time-synchronized LIF characterization
  - Table-top experiment results
  - DCFT experiment results
- Conclusions & Future Work

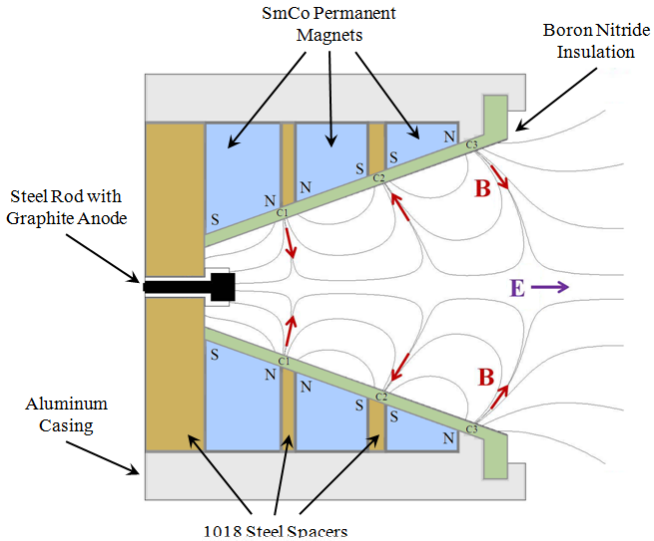

MIT Diverging Cusped Field thruster

Introduction

Motivation

- LIF velocimetry diagnostics applied to the Diverging Cusped Field Thruster (DCFT)
  - Low Current Mode
    - Quiescent, time averaged measurements are relevant
  - High current mode with
    - Strong, quasi-periodic discharge current oscillations
    - Fluctuations in position of ionization and acceleration regions
    - Dynamics not resolved with time averaged measurements
  - Discharges typically operate on xenon
    - Spectral linewidths and shifts that are too narrow to resolve with pulsed dye lasers

Laser Induced Fluorescence

- Laser beam tuned across electronic transition in Xe ions

  $5d[4]_{7/2}$–$6p[3]_{5/2}$ *at 834.72 nm*

- Ions spontaneously emit photons resulting in their relaxation from its excited state to a lower state (fluorescence)

  $6s[2]_{3/2}$ –$6p[3]_{5/2}$ *at 541.92 nm*

- Fluorescence excitation spectrum = convolution of ion velocity distribution function (VDF), and transition lineshape (inc. hfs, etc.)
- Shape (broadening/shift) dominated by Doppler effect

Approaches to Time-Synchronization

Option 1:

- Use pulsed laser to make time resolved LIF measurements

Issues:

- Typical linewidth of pulsed laser is larger than desired
  - Pulsed Nd:Yag Pumped Dye Laser: > 1.5 GHz
  - Typical Doppler width of transition: < 2 GHz

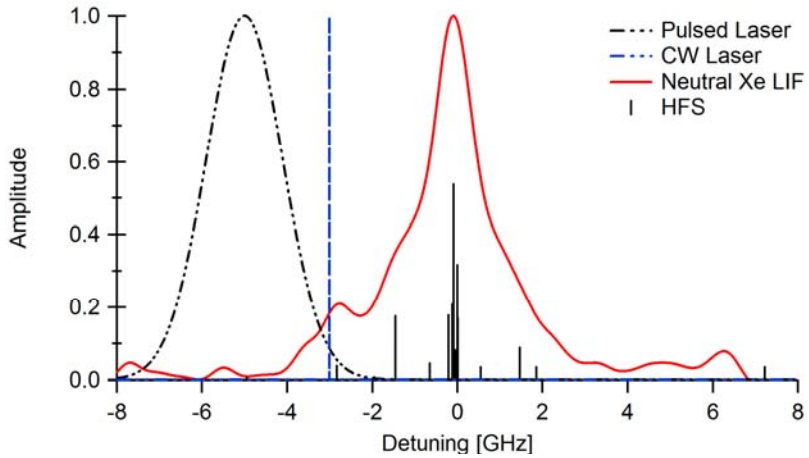

Lineshape of the 834.68 nm Xe transition compared to widths of a pulsed laser and a CW laser. Hyperfine structure (HFS) shown as reference.

Option 2:

- Use CW diode laser to take time resolved LIF measurements
  - CW Diode Laser: < 300 kHz

Approach:

- Synchronize acquisition of fluorescence signal with oscillating discharge current
- Sample-Hold Method
  - Separate out signals at different phases along current cycle
  - Uses phase-sensitive detection to remove background (allows for jitter in current frequency)

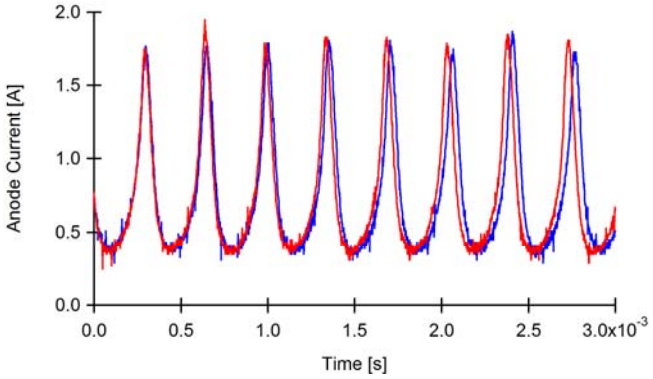

DCFT current traces, taken approx. 30 seconds apart. Note: slight change in frequency

Digital Sample-Hold Method

1. **Take simultaneous measurements of AC discharge current, emission + fluorescence**

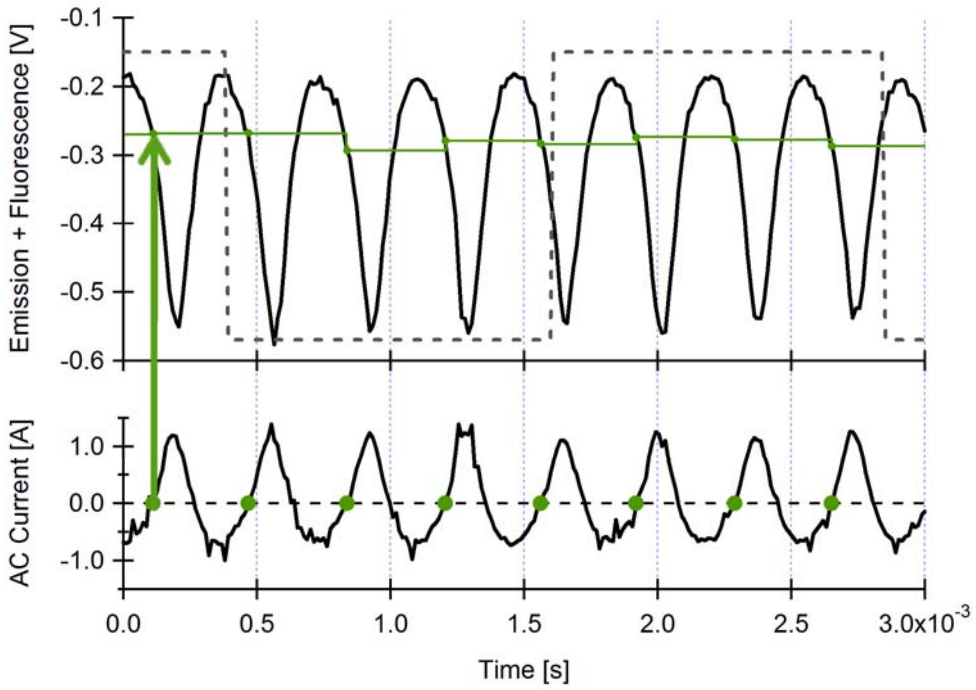

Digital Sample-Hold Method

1. Take simultaneous measurements of AC discharge current, emission + fluorescence

2. **Find zero point crossings of discharge current, mark as time=t_0**

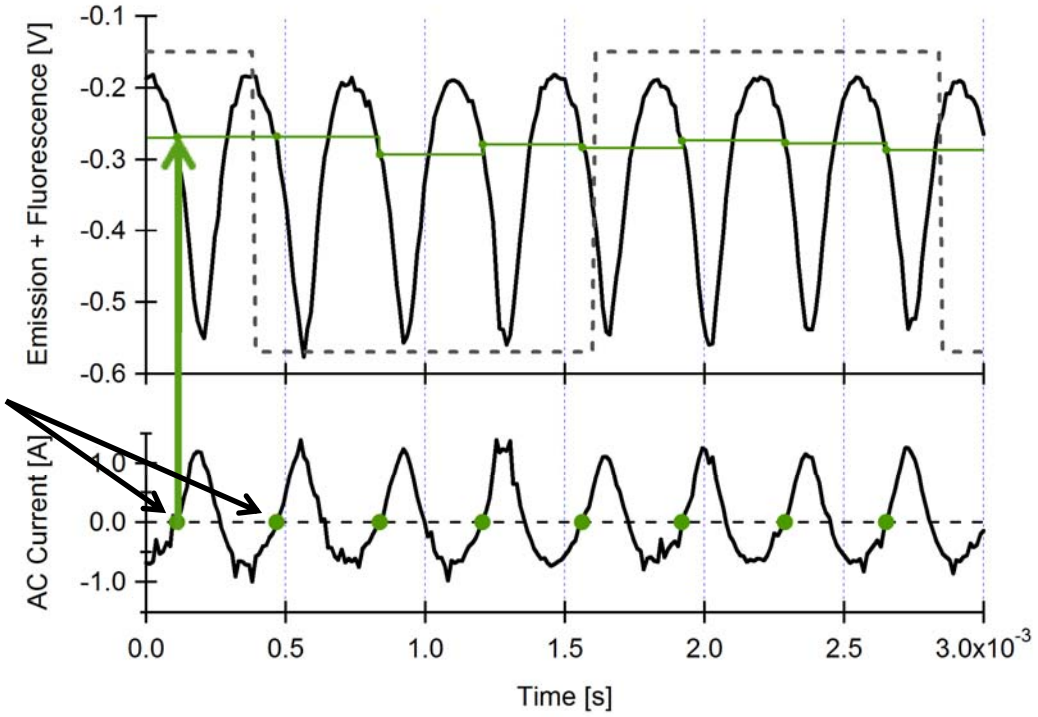

Digital Sample-Hold Method

1. Take simultaneous measurements of AC discharge current, emission + fluorescence

2. Find zero point crossings of discharge current, mark as time=t_0

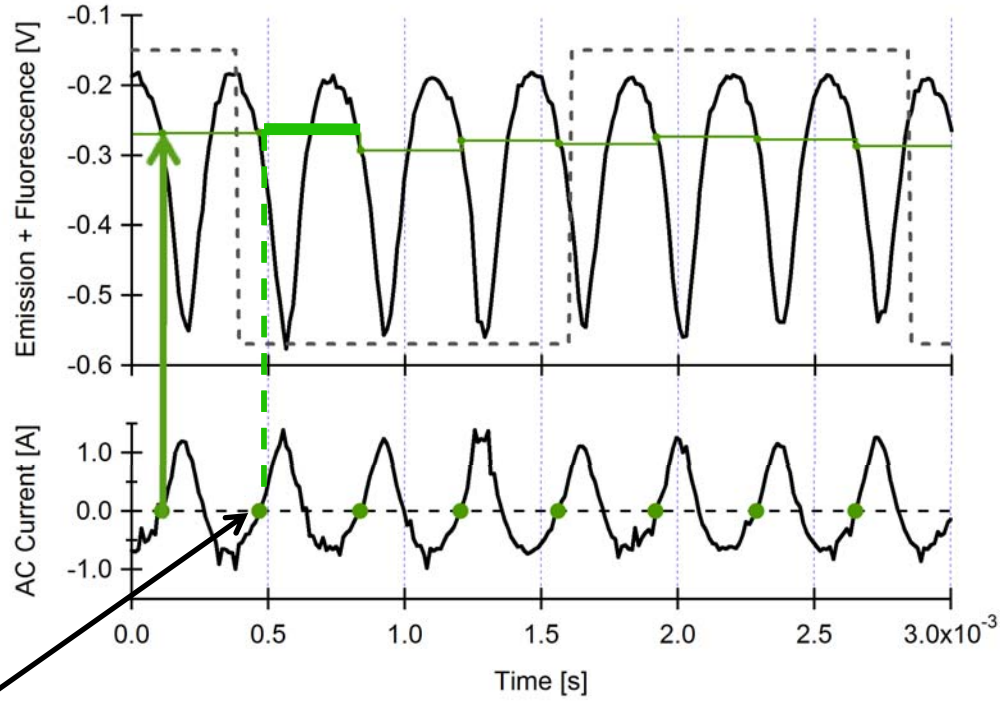

3. **Sample emission + fluorescence trace at t_0, hold value**

Digital Sample-Hold Method

1. Take simultaneous measurements of AC discharge current, emission + fluorescence

2. Find zero point crossings of discharge current, mark as time=t_0

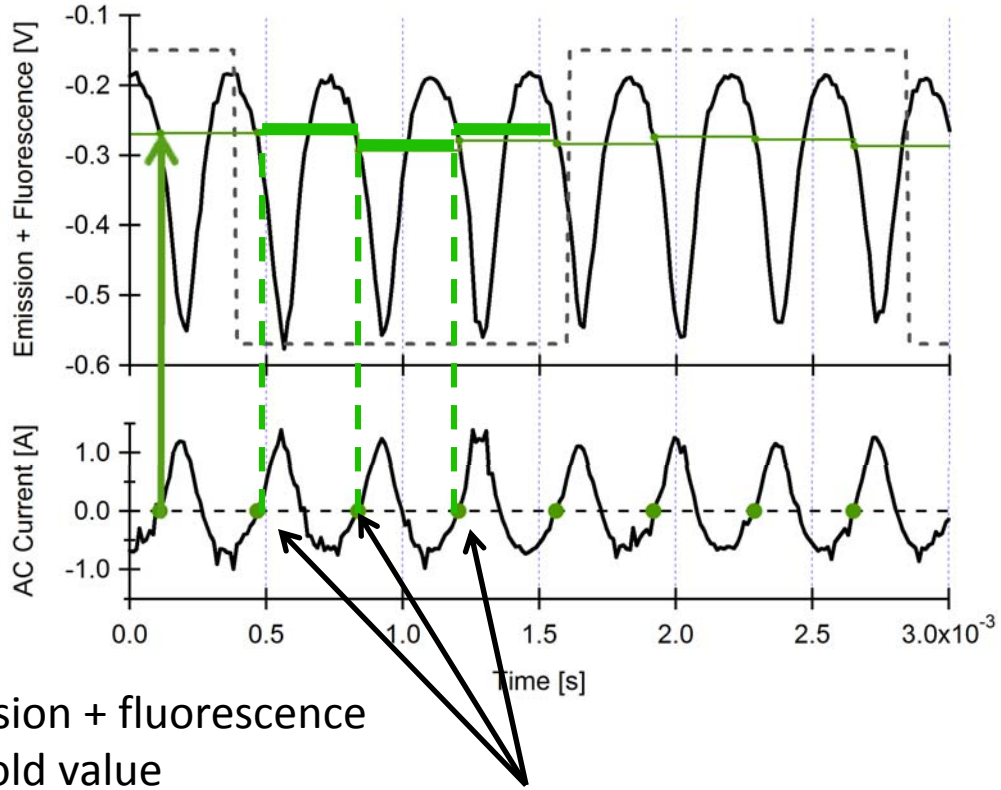

3. Sample emission + fluorescence trace at t_0, hold value

4. **Repeat sample-hold at t_0 points along entire scan**

Digital Sample-Hold Method

1. Take simultaneous measurements of AC discharge current, emission + fluorescence

2. Find zero point crossings of discharge current, mark as time=t_0

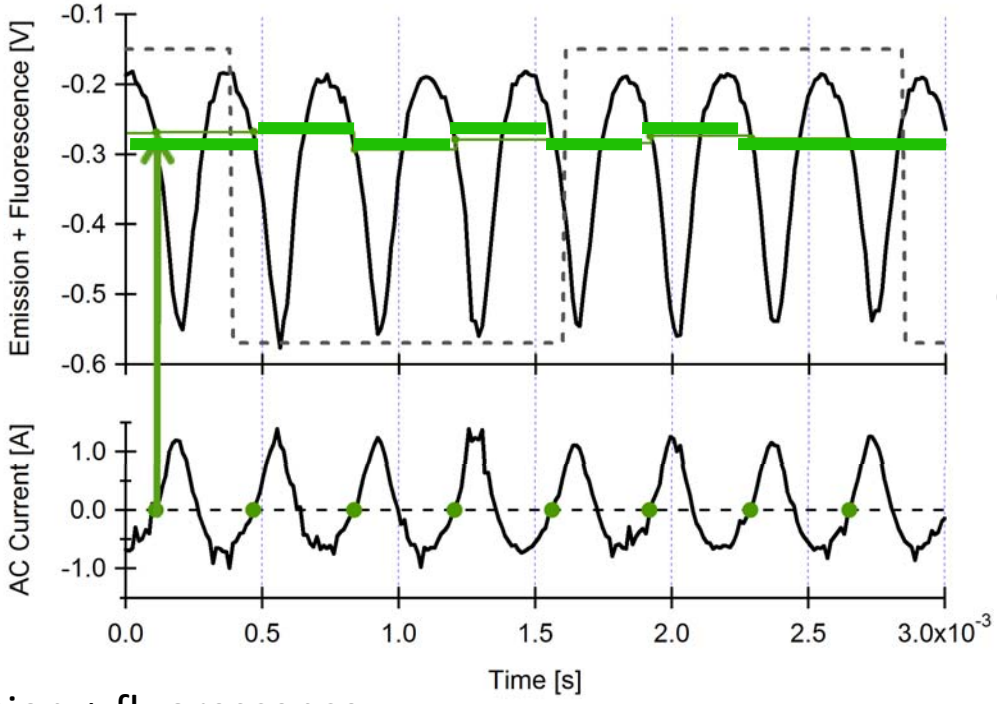

3. Sample emission + fluorescence trace at t_0, hold value

4. Repeat sample-hold at t_0 points along entire scan

5. **Pass sample-held signal through digital lock-in**

Fluorescence excitation lineshape for t_0

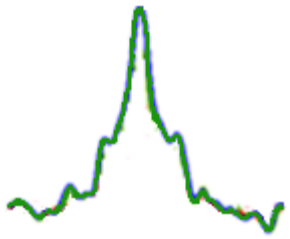

Digital Sample-Hold Method

1. Take simultaneous measurements of AC discharge current, emission + fluorescence

2. Find zero point crossings of discharge current, mark as time=t_0

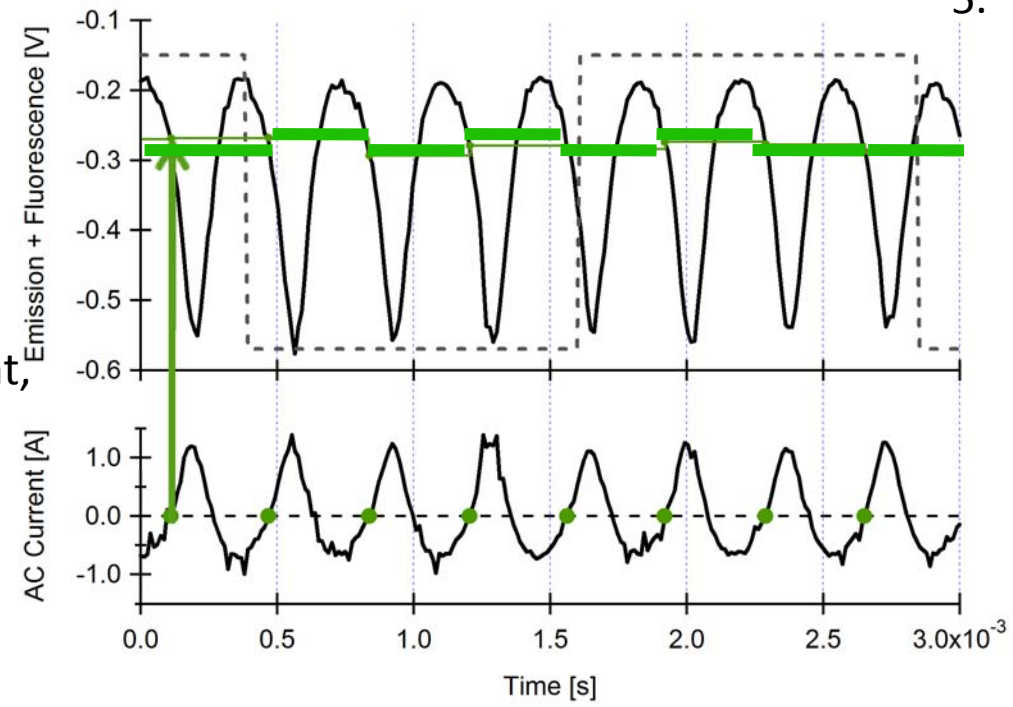

3. Sample emission + fluorescence trace at t_0, hold value

4. Repeat sample-hold at t_0 points along entire scan

5. Pass sample-held signal through digital lock-in

↓

Fluorescence excitation lineshape for t_0

6. **Repeat for t_1 , t_2, etc.**

Hardware Sample-Hold Method

1. **AC current from the discharge is fed into an LM339 comparator chip**

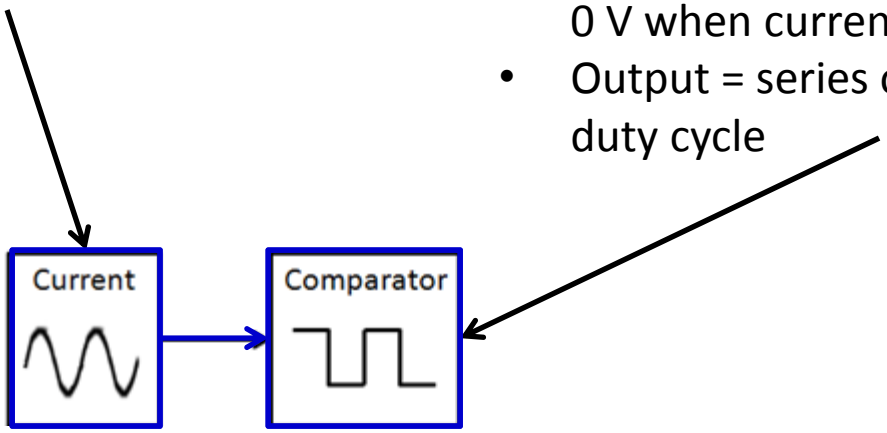

- Comparator output is +5 V when signal from current is above 0.005 V,
  0 V when current signal is below 0.005 V
- Output = series of TTL pulses with ~50% duty cycle

Hardware Sample-Hold Method

1. AC current from the discharge is fed into an LM339 comparator chip
2. **Raw emission + fluorescence trace and comparator signal sent into Stanford Research Systems SR-250 Boxcar Averager**

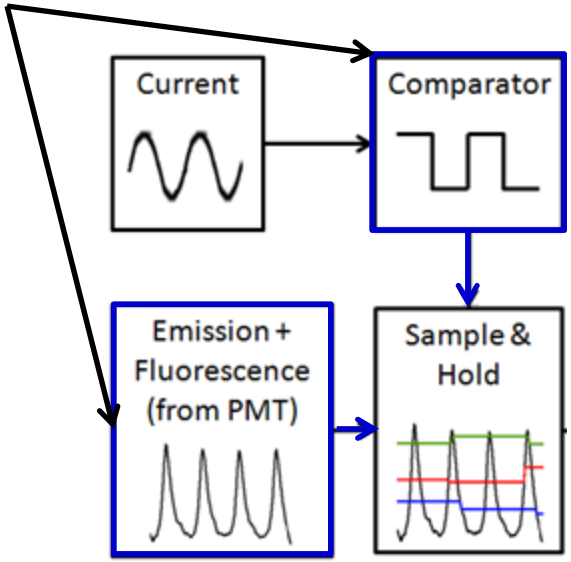

Hardware Sample-Hold Method

1. AC current from the discharge is fed into an LM339 comparator chip
2. Raw emission + fluorescence trace and comparator signal sent into Stanford Research Systems SR-250 Boxcar Averager

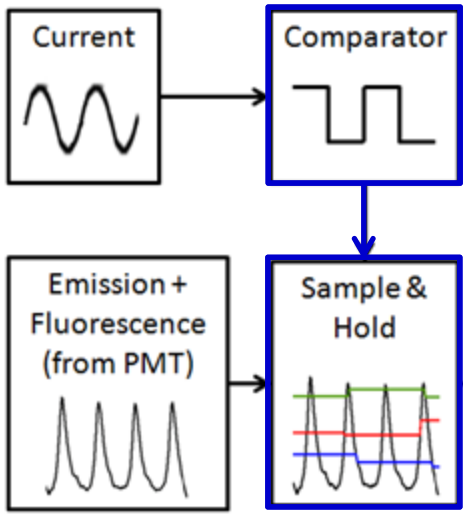

3. **TTL pulses from comparator used to trigger sample-hold function in boxcar averager for time=t_0**

Hardware Sample-Hold Method

1. AC current from the discharge is fed into an LM339 comparator chip
2. Raw emission + fluorescence trace and comparator signal sent into Stanford Research Systems SR-250 Boxcar Averager

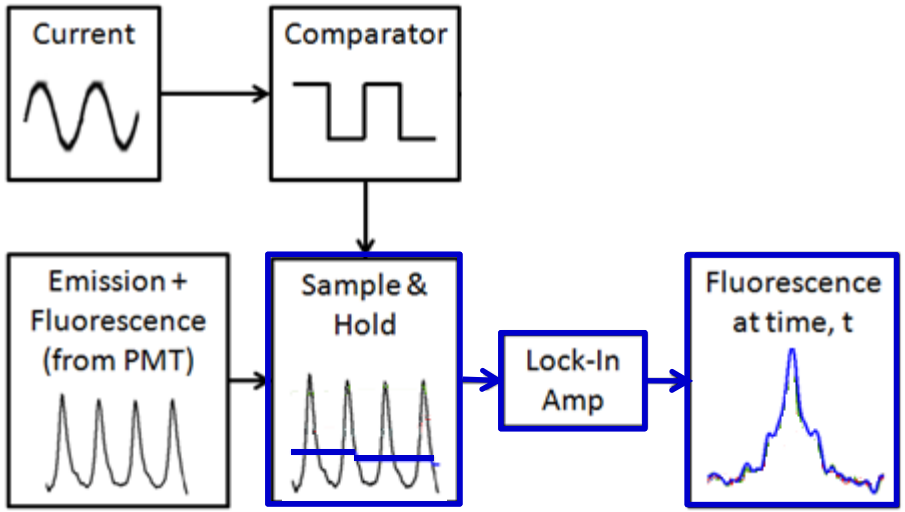

3. TTL pulses from comparator used to trigger sample-hold function in boxcar averager for time=t_0
4. **Sample-held signal from boxcar averager is sent through an SR-850 lock-in amplifier to pull out fluorescence excitation lineshape for time=t_0**

Hardware Sample-Hold Method

1. AC current from the discharge is fed into an LM339 comparator chip
2. Raw emission + fluorescence trace and comparator signal sent into Stanford Research Systems SR-250 Boxcar Averager

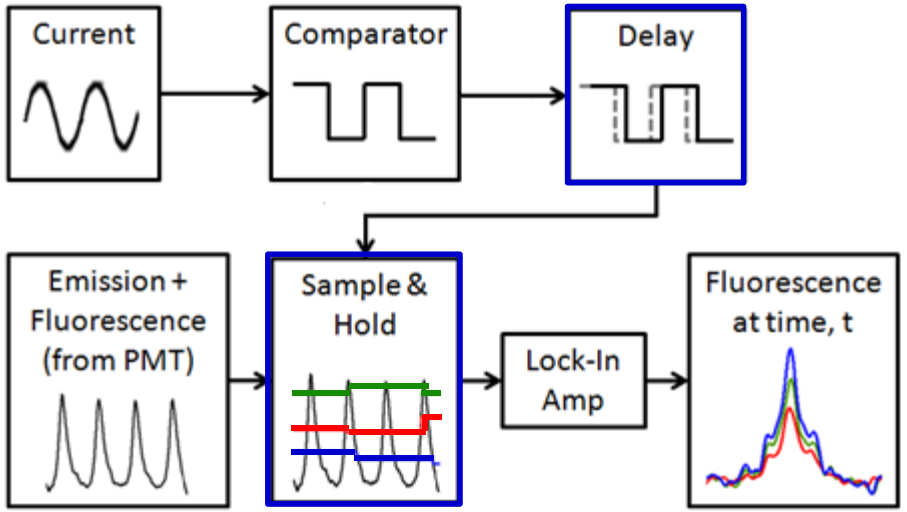

3. TTL pulses from comparator used to trigger sample-hold function in boxcar averager for time=t_0
4. Sample-held signal from boxcar averager is sent through an SR-850 lock-in amplifier to pull out fluorescence excitation lineshape for time=t_0
5. **To sample additional times along the current cycle, built in time delay in the SR-250 is used to adjust the sample trigger**

Hardware Sample-Hold Method

1. AC current from the discharge is fed into an LM339 comparator chip
2. Raw emission + fluorescence trace and comparator signal sent into Stanford Research Systems SR-250 Boxcar Averager
3. TTL pulses from comparator used to trigger sample-hold function in boxcar averager for time=t_0
4. Sample-held signal from boxcar averager is sent through an SR-850 lock-in amplifier to pull out fluorescence excitation lineshape for time=t_0
5. To sample additional times along the current cycle, built in time delay in the SR-250 is used to adjust the sample trigger

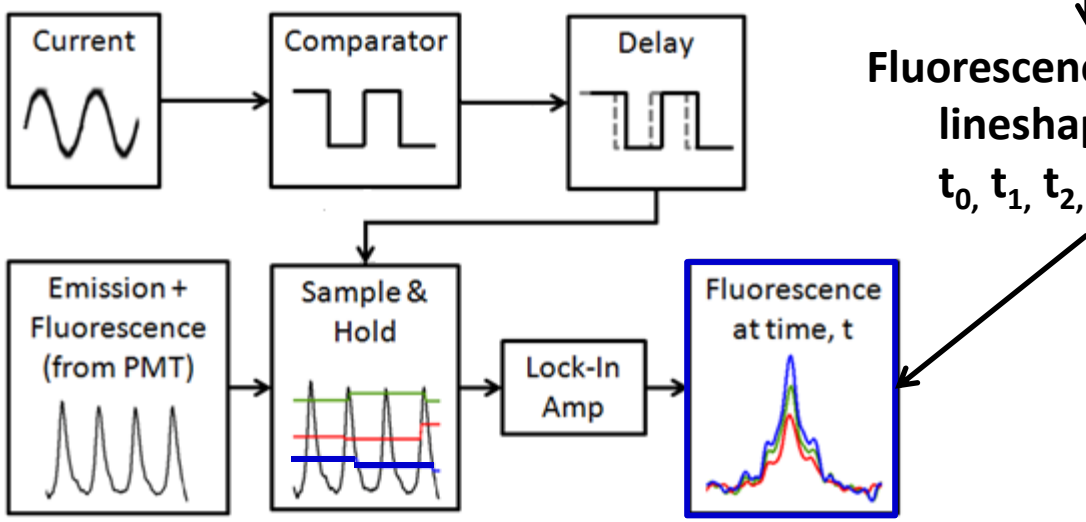

Fluorescence excitation lineshapes at time= t_0, t_1, t_2, etc.

Time-Sync DCFT Experiment

- Hardware version of sample-hold used for DCFT experiments
  - High dynamic reserve of SR-850 Lock-in Amplifier gives better noise rejection
- Xenon ion (Xe II) transition at 834.72 nm probed
  - $5d[4]_{7/2}$–$6p[3]_{5/2}$
- Non-resonant fluorescence collected at 541.92 nm
  - $6s[2]_{3/2}$ –$6p[3]_{5/2}$
- Chopper frequency at 400 Hz
  - Must be slower than discharge current frequency for sample-hold

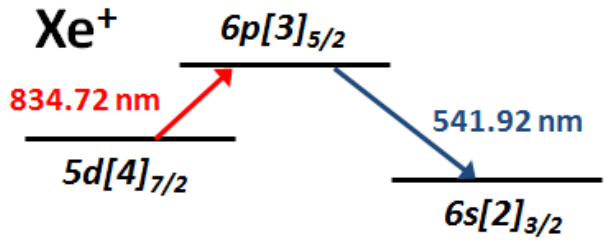

DCFT Operating Conditions	
Anode Flow Rate:	830 µg/s Xe (8.5 sccm)
Anode Potential:	300 V
Anode Current:	0.49 A
Background Pressure:	1.5×10^{-5} torr

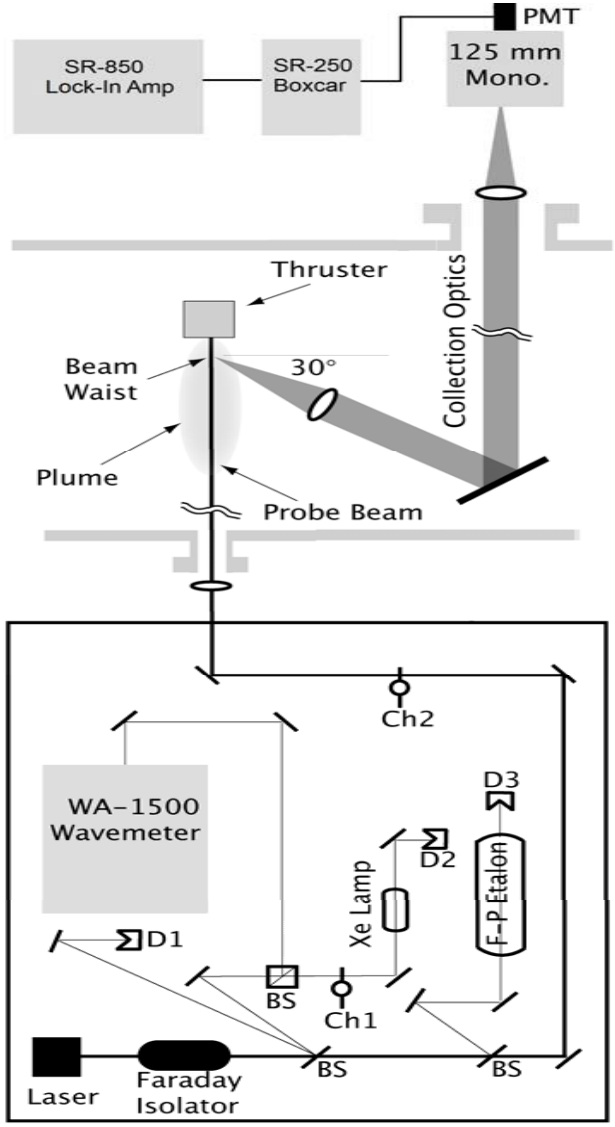

Time-Sync DCFT Results

- Time-sync LIF measurements made at the exit plane of the thruster
- Current oscillations driven by accumulation and expulsion of ions within the thruster channel
- Beginning of current cycle -- lineshape is relatively narrow, peak velocities ~5-5.5 km/s.
- Peak of current cycle -- second peak forms in velocity distribution, indicating the presence of near zero and negative velocity ions.
- End of current cycle -- second peak diminishes until the distribution resembles that beginning of the current cycle

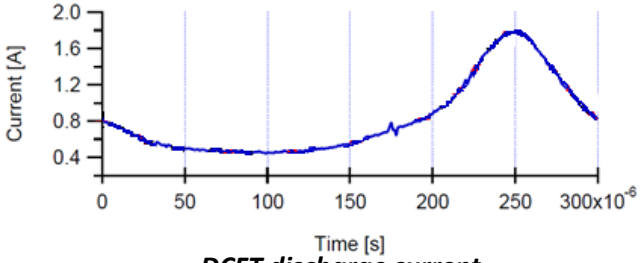

DCFT discharge current

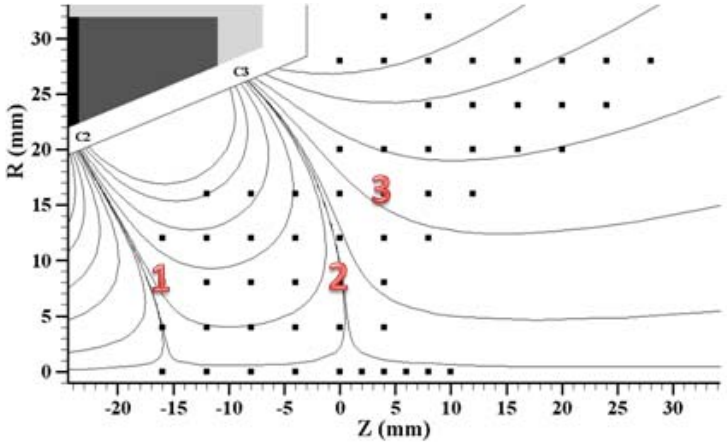

Diagram of DCFT, including location measurement

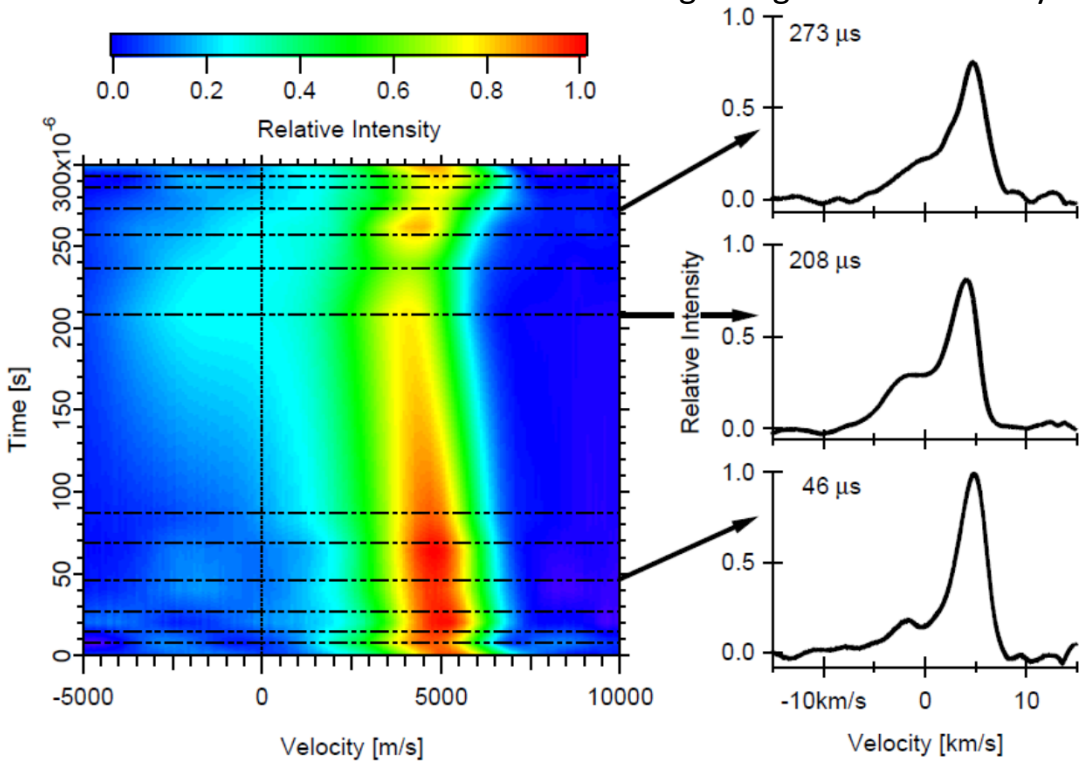

Variation of Xe ion velocity distributions for a single current cycle

Modeling of Time-Sync Results

- Simplified, 1-D simulation of ionization and acceleration
  - **F** = *q***E**, magnetic field term is neglected
  - Position and velocity of ions marched forward in time with a 4th order Runga Kutta scheme with an adaptive timestep
- Ions released at positions that oscillate between Z = -21 and -10 mm
  - In phase with the current fluctuations
  - Matches depth of ionization region seen in time-averaged velocity measurements
- Time varying electric field established by a 300 V potential drop
  - Potential drop oscillates in position near the exit plane
  - Also proportional to the current fluctuations
  - Drop is modeled by the applied anode potential minus a sigmoid function

$$\Phi(z,t) = \Phi_0(t)\left(1 - \frac{1}{1 + exp^{-w(t)z + z_0(t)}}\right)$$

  - $w(t)$ and $z_0(t)$ are time varying width and center position of potential drop
  - z_0 fluctuates between Z = -5 and +2 mm, matching acceleration region seen in time-averaged measurements

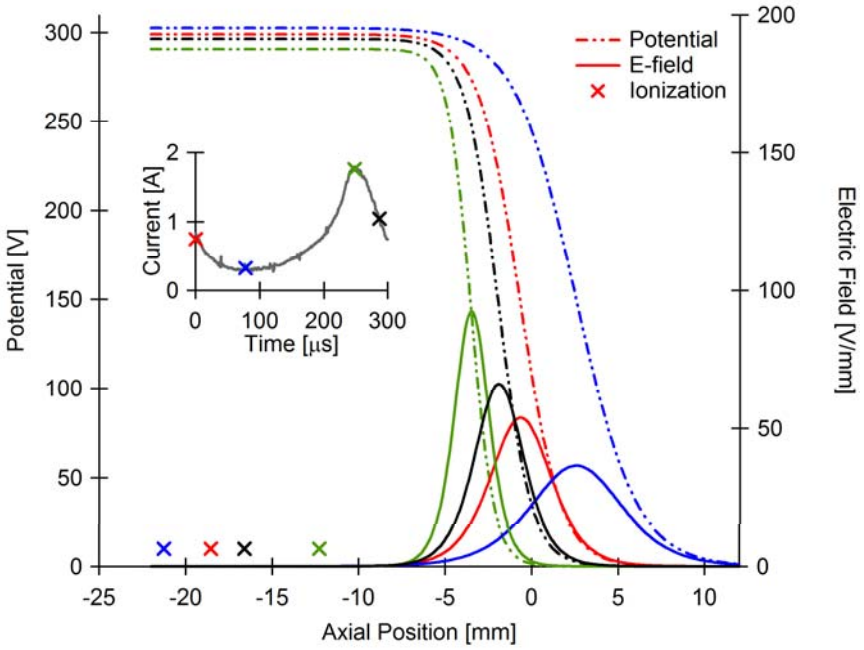

1-D simulation of discharge current oscillations

Analysis of DCFT Results

Most Probable Velocities

- Simulation is able to closely match the time-synchronized most probable velocities
- Dip in ion velocity seen at the current peak
  - Associated with the distance between ionization front and peak electric field being at a minimum
  - Ions born closer to the exit plane have traveled through less potential drop than those born closer to the anode

Width of Velocity Distribution

- Secondary velocity peak between 200-250 μs (previous slide)
  - Increases width of distribution
  - Attributed to the ions born closer to the exit plane
  - Movement of the potential drop back and forth over the measurement point may induce some backwards movement of newly born ions at exit plane
- As the neutral density is consumed, and the ionization front recedes, the width of the velocity distribution decreases
  - Low velocity second peak disappears
  - Narrowing of the ionization region eliminates negative velocity ion population

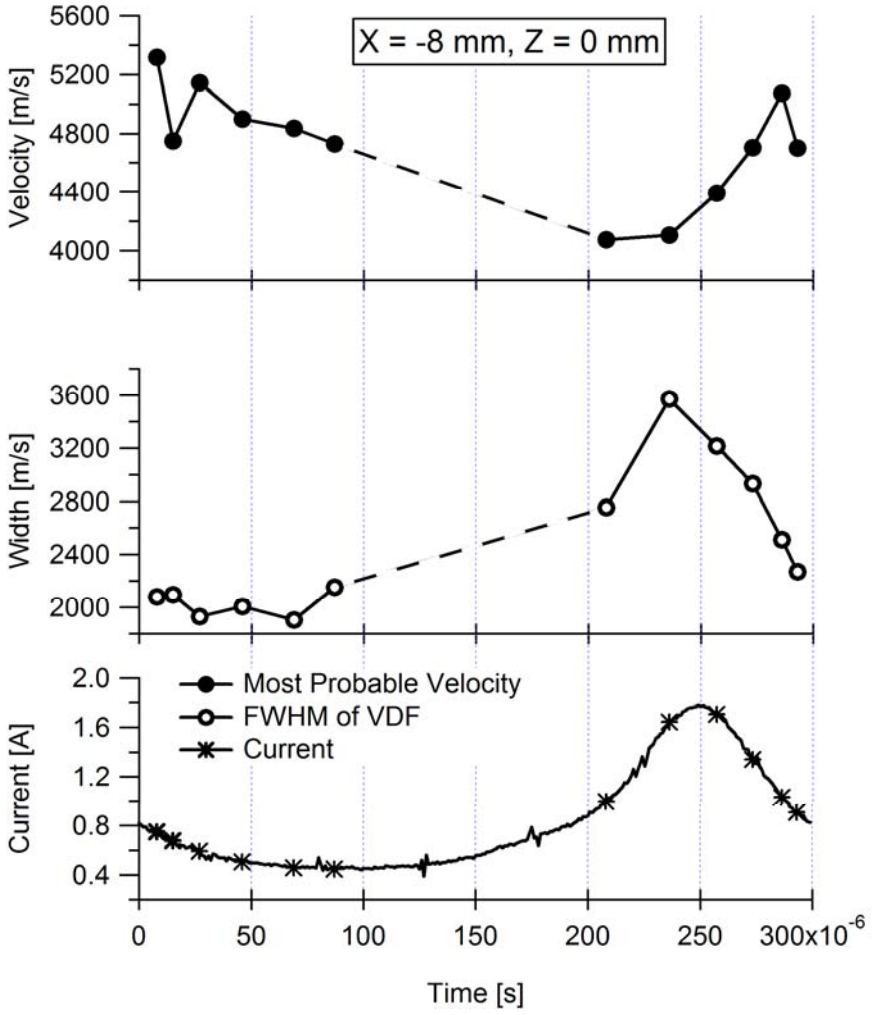

Analysis of DCFT Results Cont…

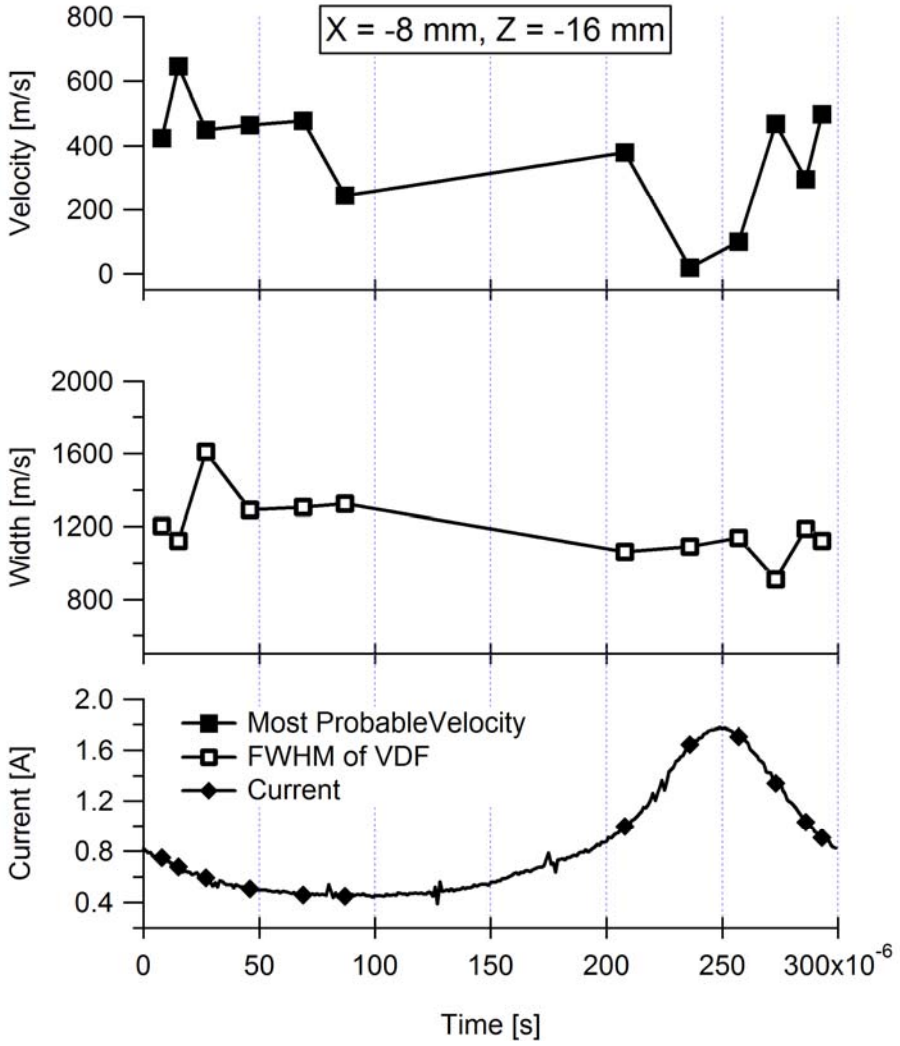

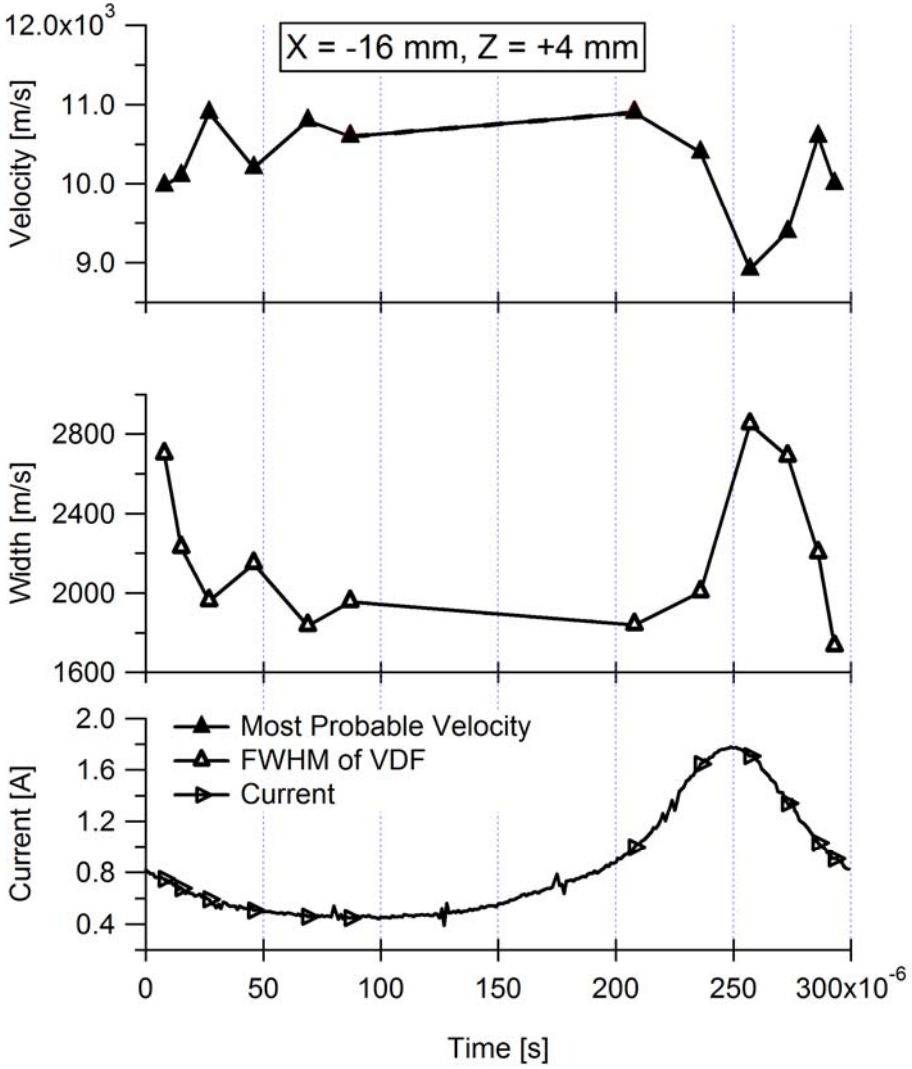

Summary

- Sample & hold/phase sensitive detection method has been implemented in software and hardware to synchronize fluorescence signal to discharge current
- Table-top measurements on Xe spectral lamp validated method for both software and hardware versions of sample-hold
- For DCFT, ion velocities appear directly related to a shifting in position of both the ionization front and acceleration regions, correlated in time with the discharge current fluctuations
- Current oscillations appear similar to a breathing mode seen in Hall thrusters

Future Work

- Increase S/N for time-sync on the DCFT by using higher power laser and faster optics
- With increased S/N, make more extensive (spatially) measurements throughout the plume of the DCFT
- Time-synchronized LIF measurement could be applied to other quasi-periodic discharges in fields such as combustion, materials processing, etc.

Thank You!

- Air Force Research Laboratory, Edwards AFB
  - Dr. Bill Hargus Jr.

Collaborations with:

- Stanford Plasma Physics Laboratory
  - Prof. Mark Cappelli

Funding through:

- Air Force Office of Scientific Research, under grant monitor Dr. M. Birkan

Back-up Slides

Why Sample-Hold?

Boxcar Averager

- Boxcar averager method is more similar to previous studies, including measurements of velocity or energy distributions in:
  - Hall thruster[1]
  - Magnetic field reconnection in a toroidal shaped plasma device[2]
  - Helicon generated pulsed argon plasma[3]
- In previous studies, plasma discharge was driven at a particular frequency
- DCFT is naturally *quasi*-periodic
  - Straight addition and subtraction of current cycle signals are not effective
  - Signals have to be stretched or interpolated such that they cover the same amount of time, introducing error

Sample-Hold

- Phase sensitive detection allows for jitter in frequency of discharge current
- Sample-hold method can get good result with fewer scans
- For small signals that can't be pulled out by boxcar averager method or digital lock-in, hardware version of sample-hold is available
  - High dynamic reserve of SR-850 Lock-In

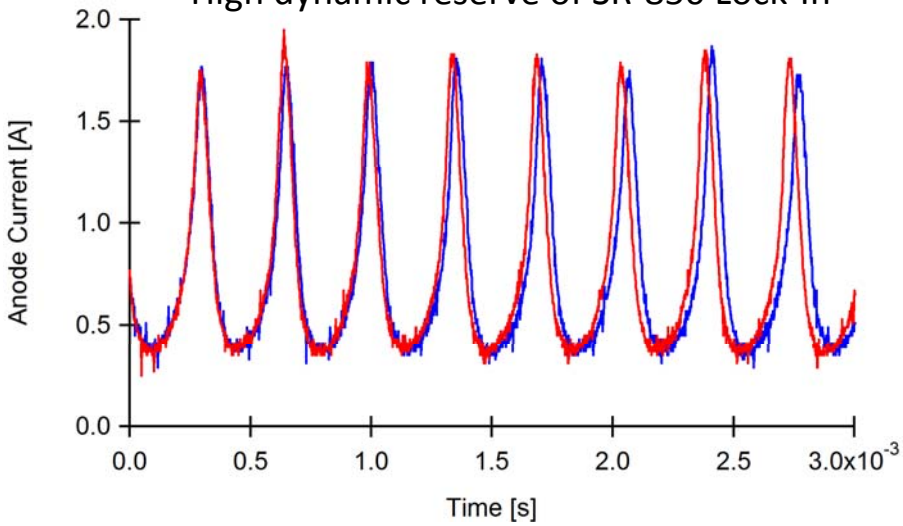

DCFT current traces, taken approx. 30 seconds apart. Note: slight change in frequency

References:

1. S. Mazouffre, D. Gawron, and N. Sadeghi. Phys. of Plasmas **16**, 1 (2009).
2. A. Stark, W. Fox, J. Egedal, O. Grulke, and T. Klinger. Phys. Rev. Lett. **95**, 1 (2005).
3. I. A. Biloiu, X. Sun, and E. E. Scime. Rev. Sci. Instrum. **77**, 10F301-1 (2006).

Gated Integration vs. Phase Sensitive Detection

Note: For CW-LIF, mechanical chopper is used to modulate frequency with a 50% duty cycle

- Phase Sensitive Detection (PSD)
  - Locks to chopper reference frequency
  - Detects average difference between signal during chopper "open" phase and background during "closed" phase
  - Maintains noise rejection even if there is jitter in background frequency

- Gated Integration
  - Integrates signal + background during "open" phase
  - Requires active background subtraction during "closed" phase
  - More effective for small duty cycle laser modulation – e.g. for pulsed lasers – where background is only integrated over a short period
  - With 50% laser duty cycle, averaging over a large number of on/off cycles is needed to achieve similar results as phase sensitive detection

Ref: "Application Note #4: Signal Recovery with PMTs," Stanford Research Systems website, www.thinkSRS.com

Cusped Field Thrusters

- Strong magnets of alternating polarity used to form cusped magnetic field
  - Cusps trap and reflect energetic electrons
  - Portions of field lines parallel to wall
  - Electron transport across magnetic field lines is small compared to mobility along field lines
- Radial field lines seen only at magnet interfaces
  - Reduced electron flux to walls reduces sheath potentials necessary for plasma neutrality in channel
  - Minimal ion bombardment and heat dissipation to the walls
- ExB drift at cusps combined with magnetic mirroring enhance propellant ionization
- Drawbacks:
  - High plume divergence angles with radial ion velocities comparable to axial ion velocities
  - Strong magnetic fields (700 Gauss – 0.5 Tesla) may cause magnetized ions

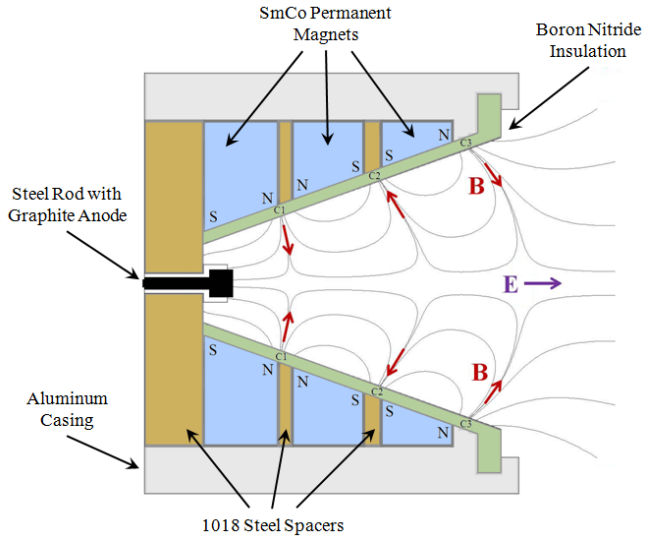

Schematic of DCFT (Ref: S. Gildea, MIT)

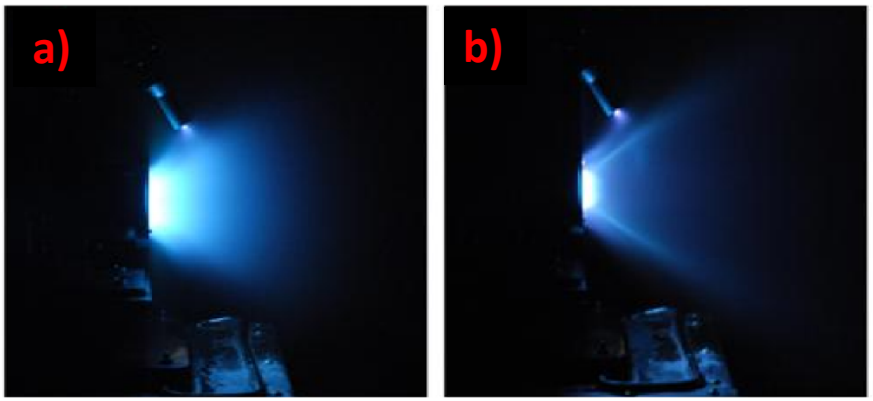

DCFT operating in: a) High current mode, b) Low current mode

Signal to Background Calculation

- Collection volume for background emission much larger than for fluorescence

$$\frac{S_f}{S_{bg}} = \frac{n_{2,f} V_f}{n_{2,bg} V_{bg}} = \frac{n_{2,f} w_L}{n_{2,bg} L}$$

$$\frac{S_f}{S_{bg}} = \frac{30 \times 10^{-6}}{0.47} = 6.4 \times 10^{-5} \qquad \frac{w_L}{L} \approx \frac{1}{10} \longrightarrow \boxed{\frac{n_{2,f}}{n_{2,bg}} = 6.4 \times 10^{-4}}$$

- Dynamic reserve of 84 dB necessary to recover fluorescence signal from background

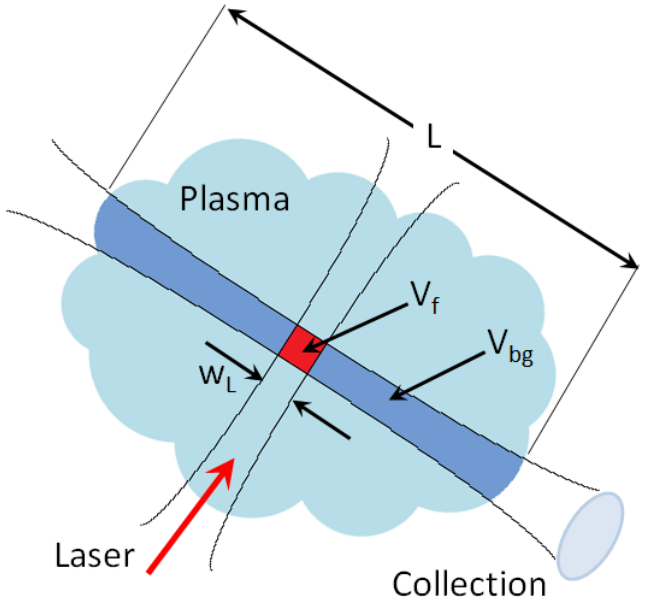

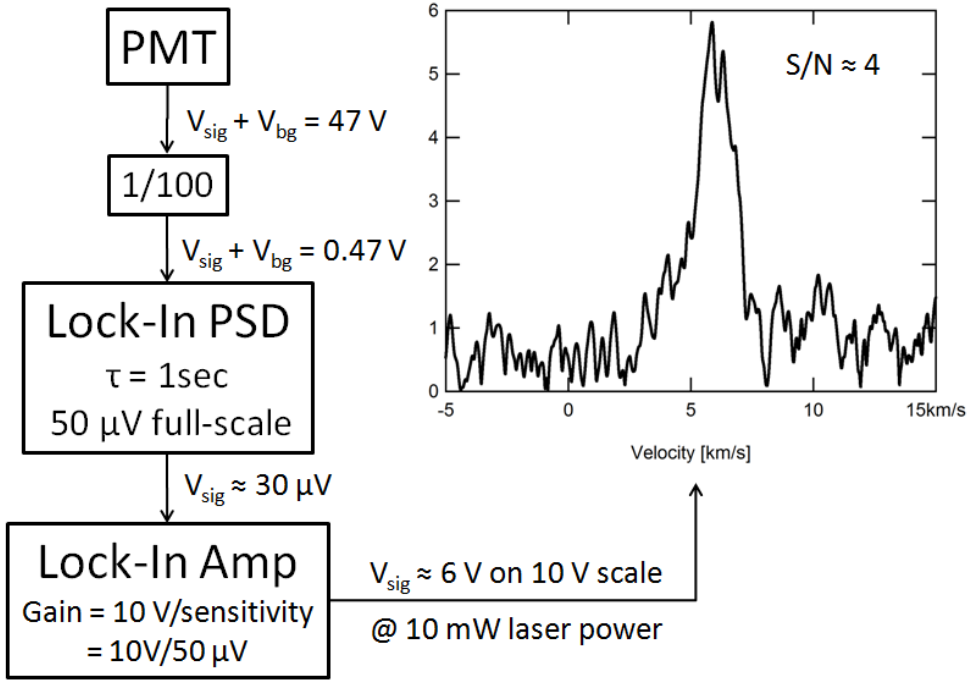

Digital Sample-Hold Method

- Simultaneous measurements of discharge current, emission + fluorescence
- Zero point crossings of discharge current with positive slope are located
  - Crossing points considered as time = t_0
  - Times t_1 , t_2 , etc. determined based on a delay time with reference to the t_0 points
- Emission plus fluorescence trace is sampled at the first data point corresponding to time = t_0
- This value is held until the current cycle reaches its next positive zero crossing
- Emission plus fluorescence trace is re-sampled and held until the next crossing
- This process is repeated for times t_1, t_2, …, splitting emission plus fluorescence trace into N separate signals corresponding to N times within the current cycle

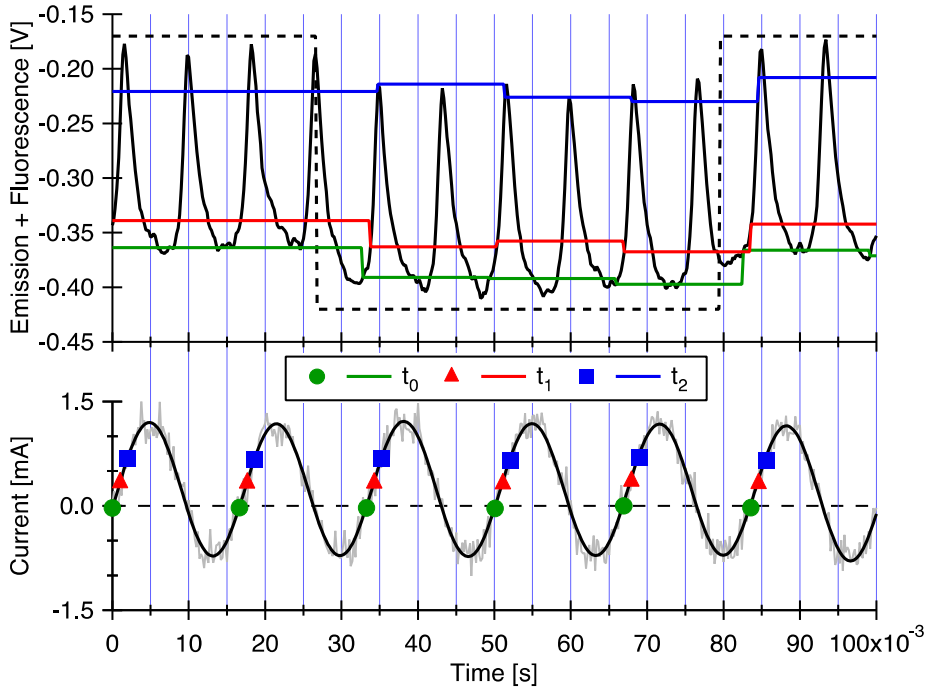

Discharge current, with points for time t_0 through t_2 (bottom). Raw PMT signal ---, chopper on/off - - -, and sample-held signals for t_0 through t_2 (top).

- The individual sample-held signals are passed through digital lock-in amplifier to pull out time-synchronized fluorescence excitation lineshapes

Hardware Sample-Hold Method

- AC current from the Xe lamp discharge is fed into an LM339 comparator chip
  - Comparator output is +5 V when signal from current is above 0.005 V, and 0 V when below
  - Comparator is configured with a hysteresis circuit to prevent over-triggering
  - Output of comparator is a series of transistor-transistor logic (TTL) pulses with ~50% duty cycle
- TTL Pulses from comparator trigger sample-hold on a Stanford Research Systems SR-250 Boxcar Averager
  - Other SR-250 inputs/settings:
    - Raw emission plus fluorescence from PMT
    - Gate width = 15µs
    - Delay time = 0 to 160 ms
  - Positive slopes in TTL trigger the boxcar averager to sample the PMT signal for a period of time defined by the gate width
  - The last sampled value of the PMT signal is held until the next TTL trigger
  - Boxcar averager re-samples the PMT signal and holds the value again

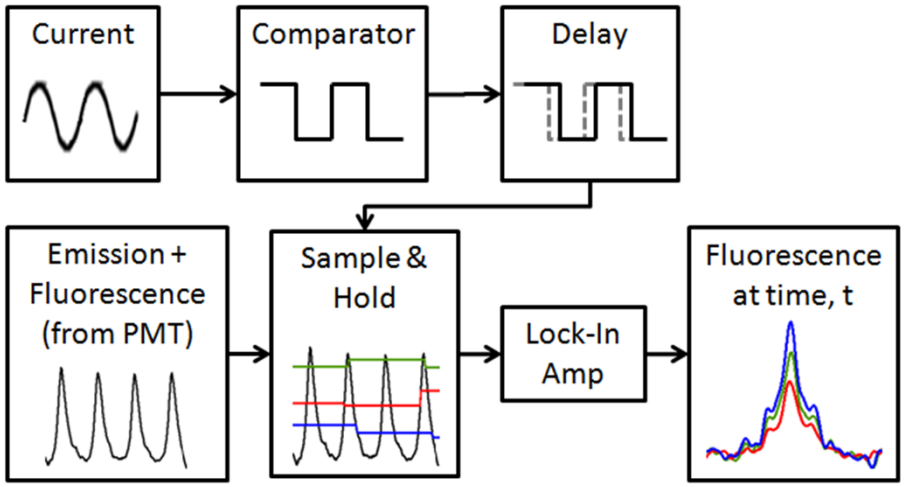

Block diagram of hardware sample-hold method

- Sample-held output is fed directly into an SRS SR-850 Lock-in Amplifier
  - Phase sensitive detection at chopper reference frequency
  - Output is a fluorescence excitation lineshape synchronized to time t_0 in the current discharge cycle
- To sample additional times along the current cycle, built in time delay in the SR-250 is used to adjust the sample trigger

Pressure vs. Broadening in Xe Lamp

- From Cedolin thesis
  - Voigt parameter, a = 2.7 in our lamp corresponds to ≈ 7 torr

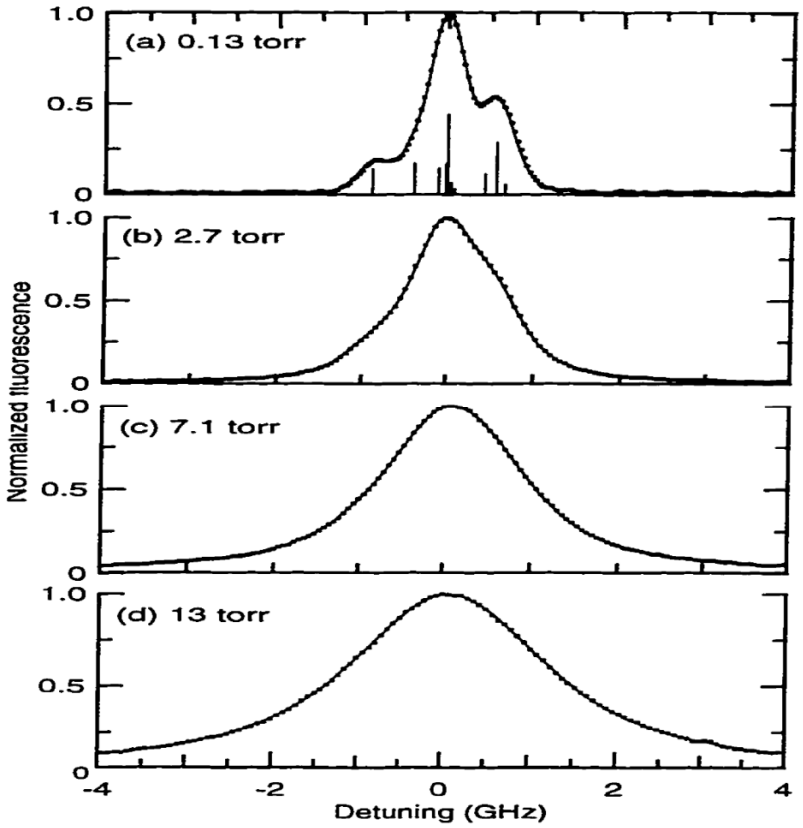

FIG. 4-4. Evolution of reduced 828-nm LIF excitation line shapes (•) and curve-fit results (—) with density: (a) 3.9×10^{21} atoms m^{-3} with contributing hyperfine lines (l), only every sixth point plotted for clarity, Voigt $a = 0.16$; (b) 8.4×10^{22} atoms m^{-3}, every tenth point plotted, $a = 1.2$; (c) 2.2×10^{23} atoms m^{-3}, every tenth point plotted, $a = 2.8$; (d) 4.0×10^{23} atoms m^{-3}, every twenty-fifth point plotted, $a = 4.9$.

Air Force Research Laboratory

Integrity ★ Service ★ Excellence

Time Synchronized CW-Laser Induced Fluorescence Measurement for Quasi-Periodic Oscillatory Plasma Discharges

Date: 29 April 2013

Natalia A. MacDonald, PhD
Research Engineer
AFRL/RQRS

Motivation

- LIF velocimetry diagnostics applied to the Diverging Cusped Field Thruster (DCFT)
  - Low Current Mode
    - Quiescent, time averaged measurements are relevant
  - High current mode with
    - Strong, quasi-periodic discharge current oscillations
    - Fluctuations in position of ionization and acceleration regions
    - Dynamics not resolved with time averaged measurements
  - Discharges typically operate on xenon
    - Spectral linewidths and shifts that are too narrow to resolve with pulsed dye lasers

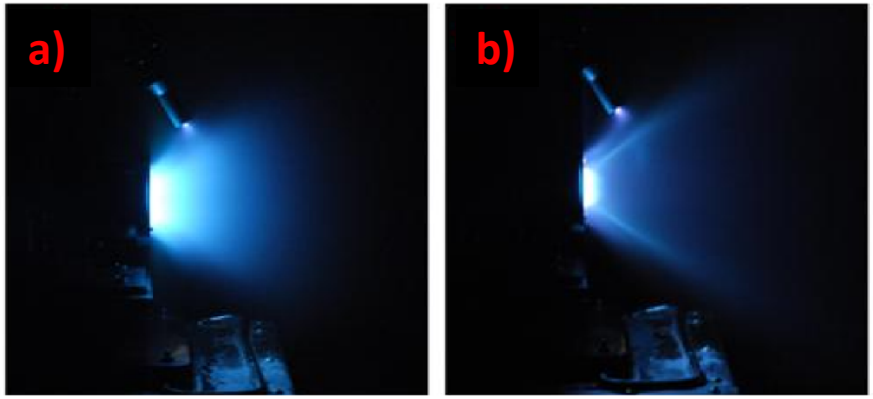

DCFT operating in: a) High current mode, b) Low current mode

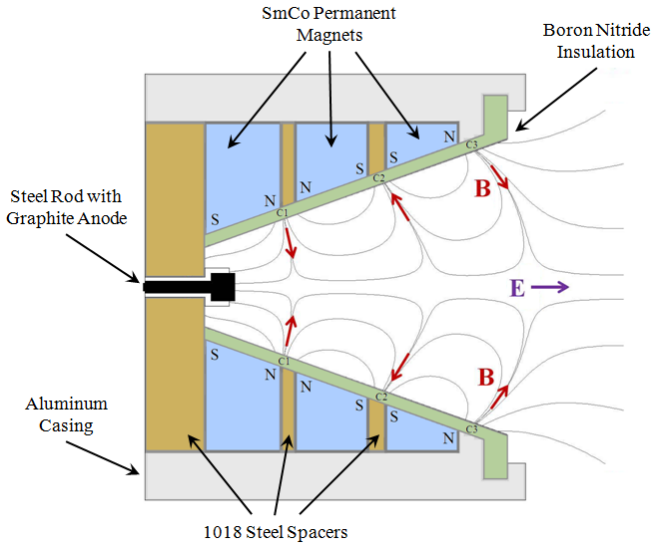

Schematic of DCFT

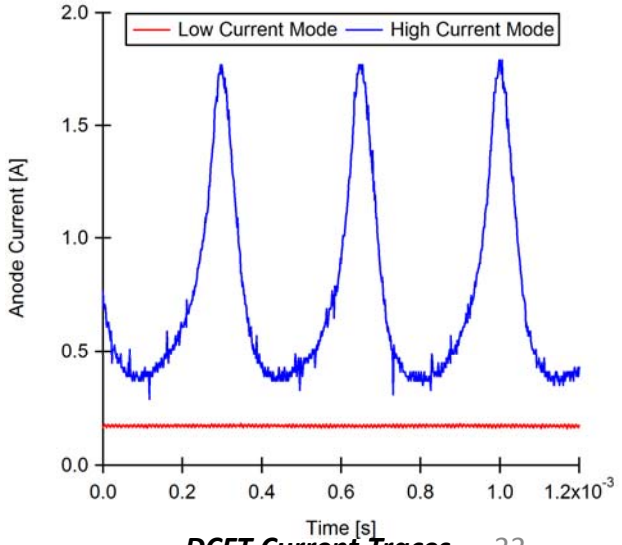

DCFT Current Traces

Laser-induced Fluorescence Velocimetry

LIF is used to measure the velocity of ions in the thruster plume

- Laser beam tuned across electronic transition in Xe ions

  $5d[4]_{7/2}$–$6p[3]_{5/2}$ *at 834.72 nm*

- Ions spontaneously emit photons resulting in their relaxation from its excited state to a lower state (fluorescence)

  $6s[2]_{3/2}$ –$6p[3]_{5/2}$ *at 541.92 nm*

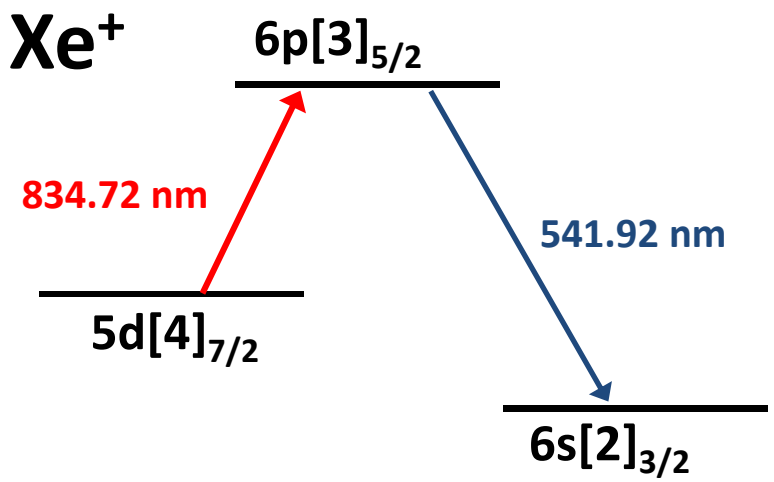

Non-resonant fluorescence scheme

- Fluorescence excitation spectrum = convolution of ion velocity distribution function (VDF), and transition lineshape (inc. hfs, etc.)
- Shape (broadening/shift) dominated by Doppler effect:

$$\delta\nu_{12} = \frac{V}{c}\nu_{12}$$

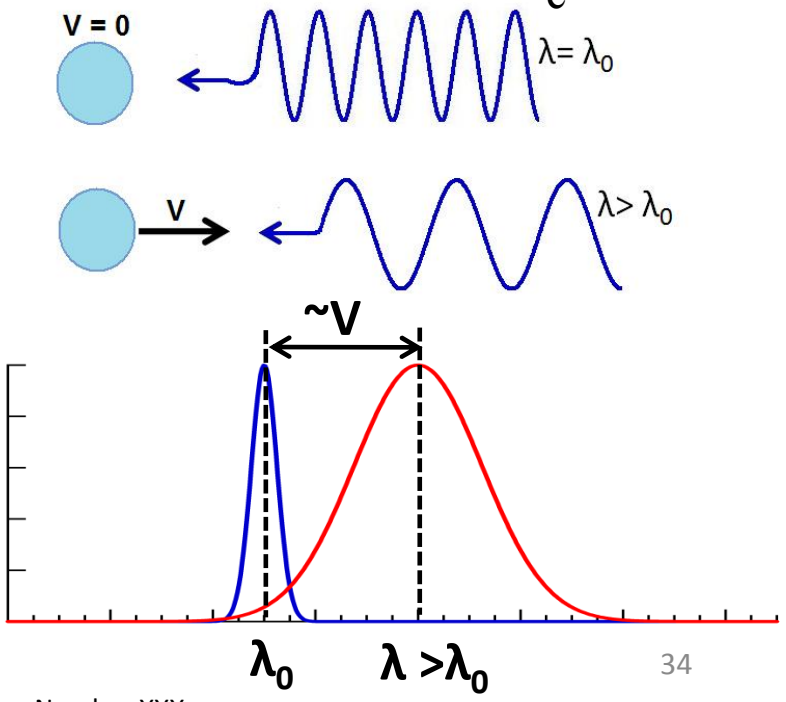

Digital Sample-Hold Method

1. **Take simultaneous measurements of AC discharge current, emission + fluorescence**

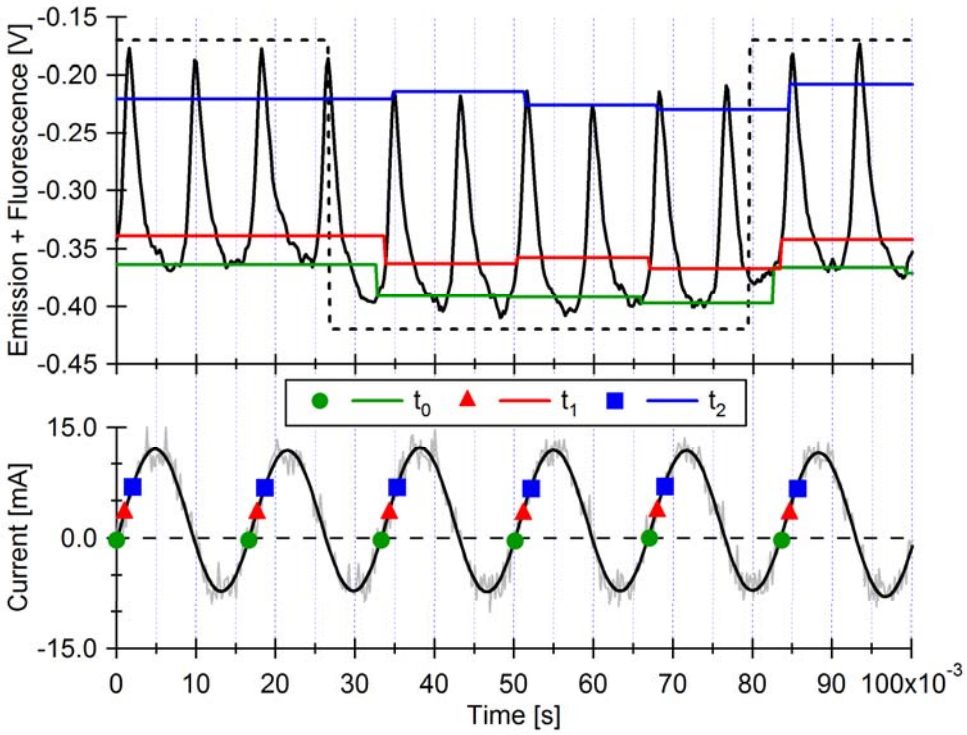

Digital Sample-Hold Method

1. Take simultaneous measurements of AC discharge current, emission + fluorescence

2. **Find zero point crossings of discharge current, mark as time=t_0**

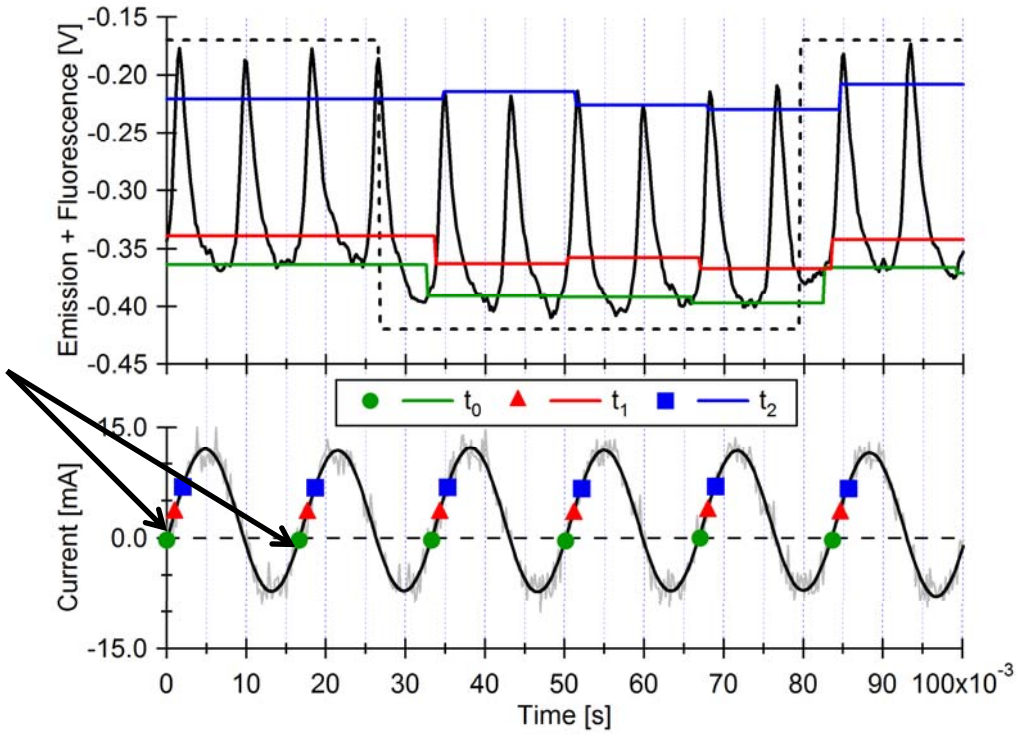

Digital Sample-Hold Method

1. Take simultaneous measurements of AC discharge current, emission + fluorescence

2. Find zero point crossings of discharge current, mark as time=t_0

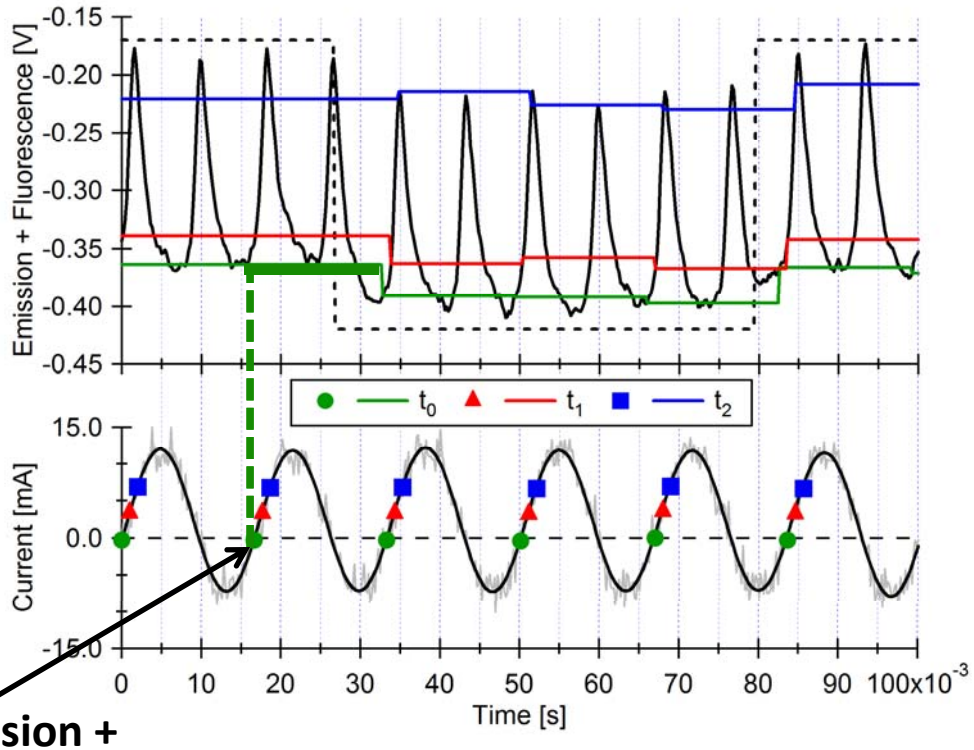

3. **Sample emission + fluorescence trace at t_0, hold value**

Digital Sample-Hold Method

1. Take simultaneous measurements of AC discharge current, emission + fluorescence

2. Find zero point crossings of discharge current, mark as time=t_0

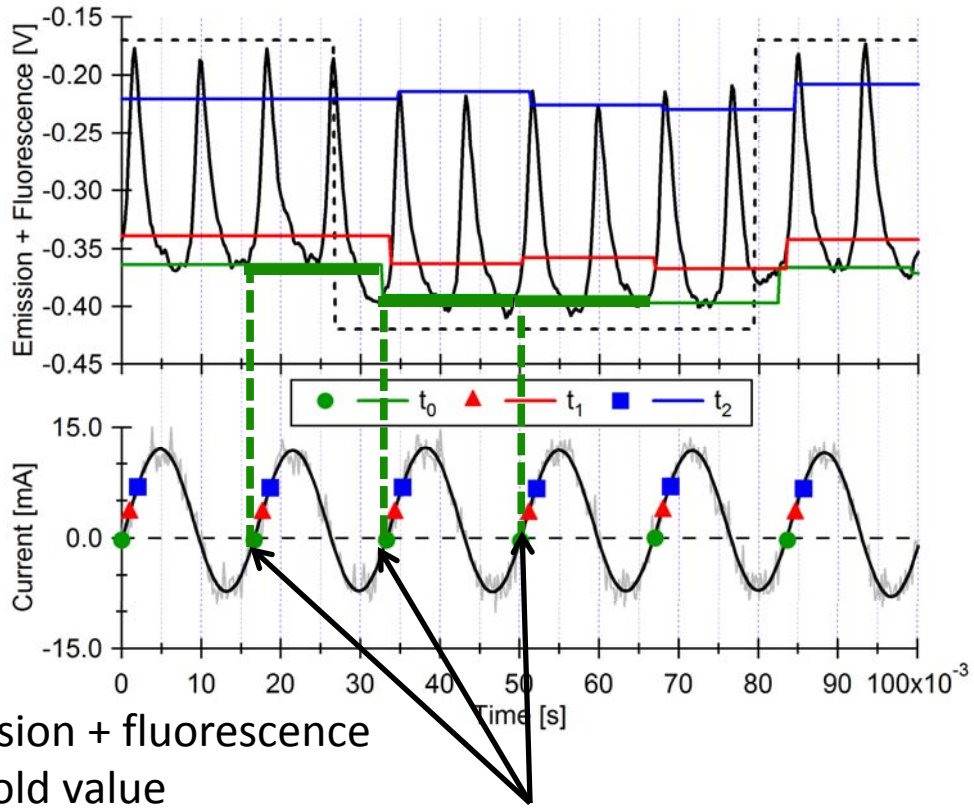

3. Sample emission + fluorescence trace at t_0, hold value

4. **Repeat sample-hold at t_0 points along entire scan**

Digital Sample-Hold Method

1. Take simultaneous measurements of AC discharge current, emission + fluorescence

2. Find zero point crossings of discharge current, mark as time=t_0

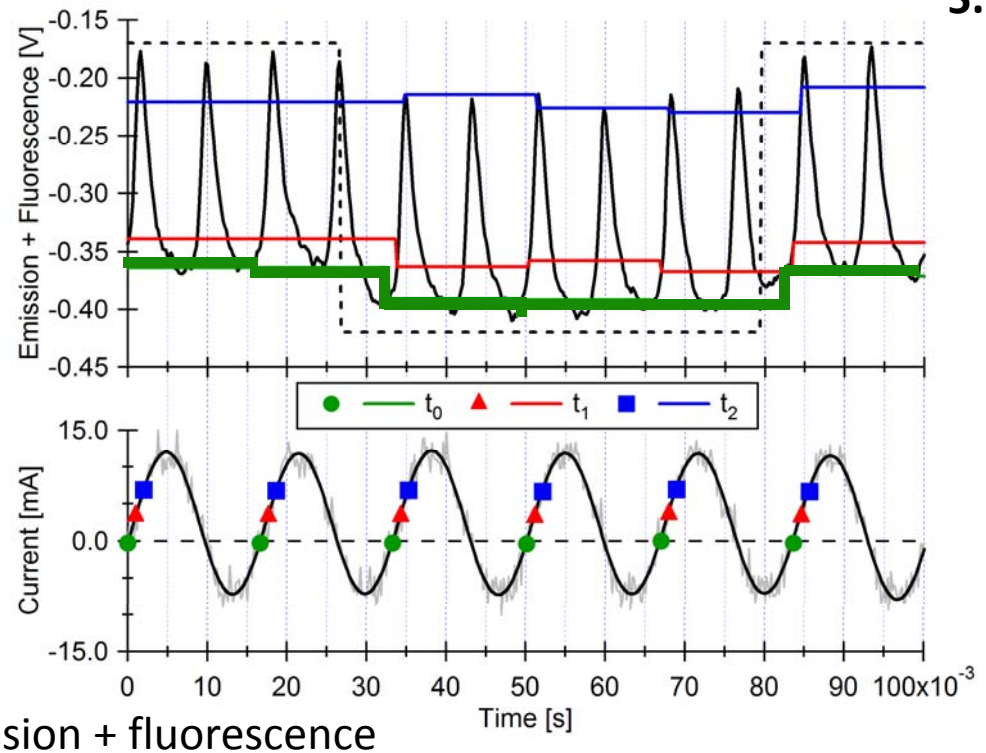

3. Sample emission + fluorescence trace at t_0, hold value

4. Repeat sample-hold at t_0 points along entire scan

5. **Pass sample-held signal through digital lock-in**

Fluorescence excitation lineshape for t_0

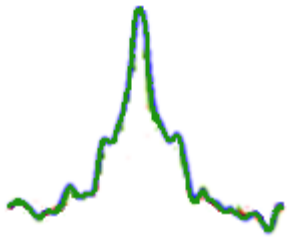

Digital Sample-Hold Method

1. Take simultaneous measurements of AC discharge current, emission + fluorescence

2. Find zero point crossings of discharge current, mark as time=t_0

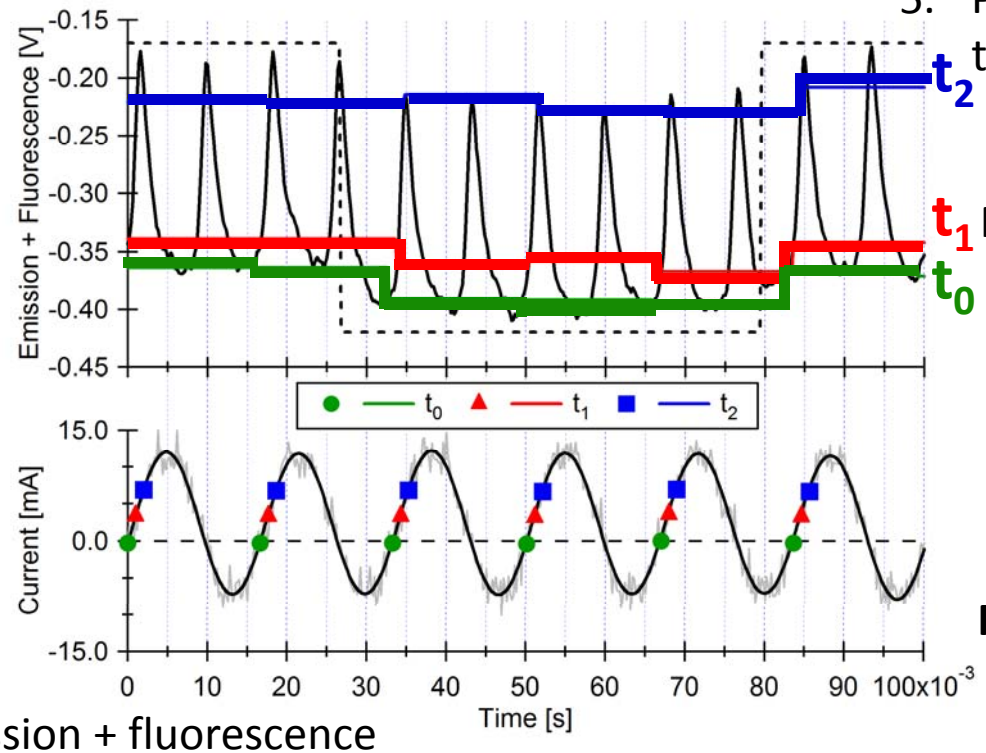

3. Sample emission + fluorescence trace at t_0, hold value

4. Repeat sample-hold at t_0 points along entire scan

5. Pass sample-held signal through digital lock-in

↓

Fluorescence excitation lineshape for t_0

6. **Repeat for t_1 , t_2, etc.**

↓

Fluorescence excitation lineshapes for t_0, t_1, t_2